The Theory of Straight Homogeneous
Generalized Cylinders
and
A Taxonomy of Generalized Cylinders

18 January 1983

Steven A. Shafer

Takeo Kanade

Computer Science Department

Carnegie-Mellon University

The Theory of Straight Homogeneous Generalized Cylinders

15 January 1983

Steven A. Shafer

Takeo Kanade

Computer Science Department

Carnegie-Mellon University

Abstract

In recent years, Binford's generalized cylinders *have become a commonly used shape representation scheme in computer vision. However, research involving generalized cylinders has been hampered by a lack of analytical results at all levels, even including a lack of a precise definition of these shapes.*

In this paper, a definition is presented for Generalized Cylinders and for several subclasses. Straight Generalized Cylinders, with a linear axis, are important because the natural object-centered coordinates are not curved. The bulk of the paper is concerned with Straight Homogeneous Generalized Cylinders, in which the cross-sections have constant shape but vary in size.

The results begin with deriving formulae for points and surface normals for these shapes. Theorems are presented concerning the conditions under which multiple descriptions can exist for a single solid shape. Then, projections, contour generators, shadow lines, and surface normals are analyzed for some subclasses of shapes. The strongest results are obtained for solids of revolution (which we name Right Circular SHGCs), for which several closed-form methods for analyzing images are presented.

Table of Contents

List of Figures

1. Introduction

In recent years, the *generalized cylinders* proposed by Binford [2] have become an increasingly important tool for shape description in image understanding. However, generalized cylinders have in the past been defined primarily in informal terms, leading to several different definitions for "generalized cylinder" (or "generalized cone") and resulting in a lack of rigorous geometric analysis of these shapes. In this paper, we present a formal definition of generalized cylinders and several interesting subclasses. A number of theorems and results are then derived, including formulas for the coordinates of the constituent points and surface normals, and several results relevant to projections (i.e. images) of generalized cylinders.

1.1 Importance of Generalized Cylinders
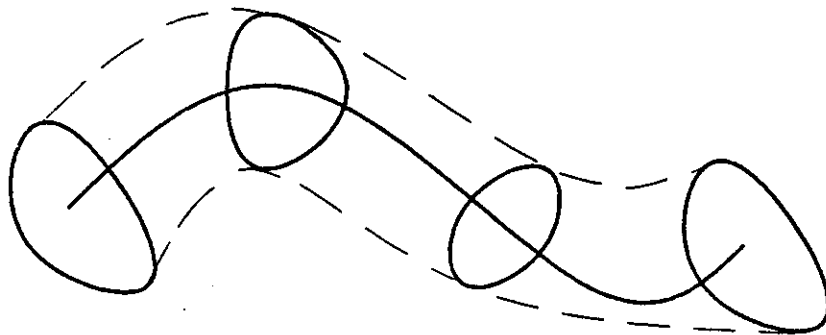
Figure 1: Concept of a Generalized Cylinder

A *generalized cylinder* is loosely characterized by having an *axis* (a space curve which forms a spine for the shape), a *cross-section* (a 2-D contour which sweeps along the axis), and a *sweeping rule* (a rule for transforming the cross-section as it is swept along the axis) (figure 1) [2].

Generalized cylinders are an important class of shapes for several reasons. They are primarily important because of the wide variety of man-made and natural objects which can be represented as generalized cylinders. For example, many objects which stand up have a vertical axis (counteracting gravity) and a horizontal cross-section which changes only slightly (if at all) as it follows the axis: a vase, a lamp, a flower stem, a skyscraper, a cup, a blade of grass, a box (figure 2). For many of these shapes, representation as a polyhedron requires defining many identical facets, which fails to take into account the simplicity of the basic structure involved. In addition, machining processes may
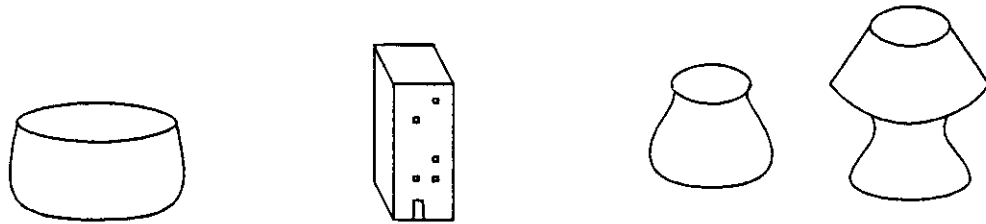
Figure 2: Examples of Generalized Cylinders

produce shapes which are rounded generalized cylinders, for which polyhedral or surface patch approximations introduce undesirable edges and corners. Generalized cylinders have been used for describing pottery types for anthropology [6] and for modelling biological cell shapes [18].
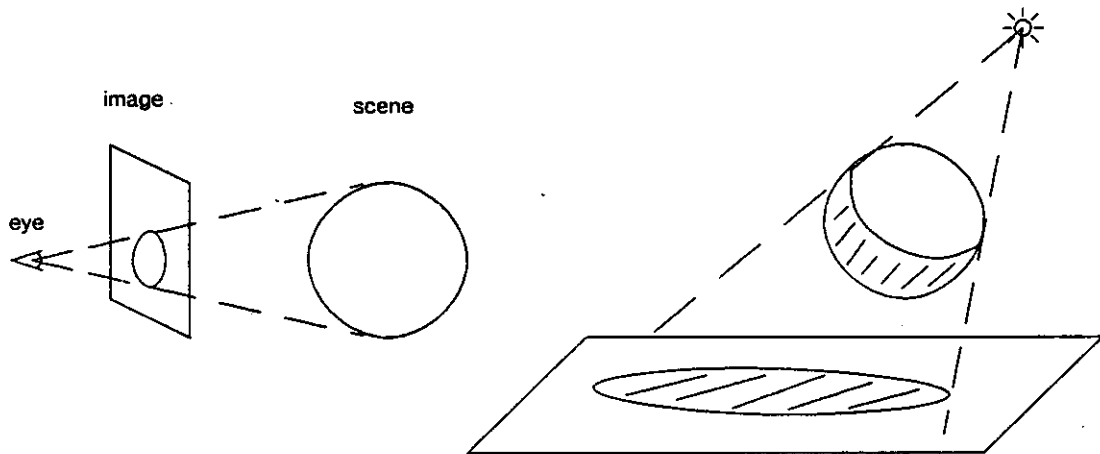
Figure 3: Imaging and Shadow Volumes are Generalized Cylinders

Generalized cylinders are important in computer image processing because of the fact that a region of an image corresponds to some volume in space, defined by the imaging projection (orthography or perspective). The volume so defined is a generalized cylinder, with axis along the optical axis of the eye or camera (figure 3). Similarly, when an object casts a shadow, there is a volume of space behind the object which will be shaded from the light source. This volume is a generalized cylinder. Thus, the problem of determining the shape of a shadow is equivalent to the geometric problem of determining the intersection of a generalized cylinder with another object (such as a planar surface).

Generalized cylinders also have several properties which render them appropriate for geometric modeling tasks, as pointed out by Marr and Nishihara [12]: generalized cylinders are *volumetric*, which means they are characterized as occupying a volume of space rather than being a collection of flat or curved patches; they have *object-centered coordinates*, which allow for rotations etc. for model instantiation or to represent motion of limbs; they have a *principal axis* which itself can be used as a gross approximation to the volume represented; and they can be *organized hierarchically* to represent coarse and fine details.

1.2 This Presentation

In this paper, we begin by defining several classes of solid shapes. Various definitions of "generalized cylinder" or "generalized cone" in the literature are identified as corresponding to certain of these classes. A particular class, called *Straight Generalized Cylinders (SGC)*, is fundamental since the natural object-centered coordinate system has no curvature in the axes, and hence is a linear transformation from world space coordinates. A subset of SGC, *Straight Homogeneous Generalized Cylinders (SHGC)*, contains those SGCs whose cross-sections have the same shape but may vary in size; this allows a decomposition of the shape description into size and shape functions, upon which this work is based. Several subclasses of SHGC are defined, with particular properties which allow stronger statements to be made about them in various situations. The remainder of the paper consists of the elaboration of important properties of Straight Homogeneous Generalized Cylinders and of these subclasses.

The next section presents the most important formulae: the coordinates of points on an SHGC, and the surface normal vector at each point. Two important problems are identified: the existence of different representations for the same solid shape, and the constancy of surface normals in certain locations. Theorems are proven in each case, showing that the *Linear SHGCs (LSHGC)* (SHGCs which expand the contour by a scaling factor proportional to distance along the axis) are a very important class by themselves. Since the imaging volumes and shadow volumes (discussed above) are LSHGCs, these results may be especially useful.

The consequences of projection of SHGCs (i.e. imaging) are then explored. This includes a general formulation of the imaging geometry, followed by an analysis of the problem of mapping image points to points on the SHGC. The analysis of silhouettes of SHGCs is explored, including the difficult problem of determing the *contour generators* -- points on the SHGC which are imaged on the outline of the silhouette [11]. Next, the problem is addressed of interpreting the contour generators from one point of view as seen from another: this arises in stereo and shadow geometry analysis. The use of range-finder data for description of SHGCs is also discussed.

2. Classes of Shapes

We will begin by defining some classes of solid shapes. We begin with *Generalized Cylinders*, which introduce the most basic ideas in the definition, then specialize this to *Straight Generalized Cylinders*, *Straight Homogeneous Generalized Cylinders*, and several subclasses of Straight Homogeneous Generalized Cylinders which we call *Linear*, *Right*, *Circular*, and *Polygonal* SHGCs. The names of these classes will be capitalized when used to refer to their formal definitions. This terminology corresponds to that of the authors in related work [16]. A summary of the symbols used will be found in an Appendix.

2.1 Generalized Cylinders
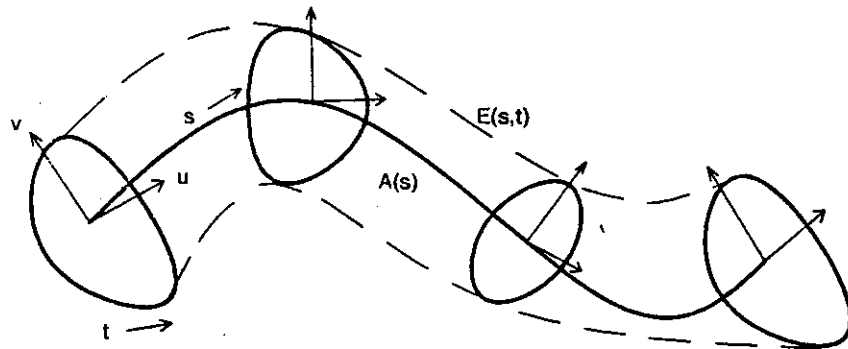
Figure 4: Generalized Cylinder

A *Generalized Cylinder (GC)*, as shown in figure 4, is a function which maps two parameters onto a set of points in x-y-z space (i.e. the world). The two parameters are s, which measures distance along the axis, and t, which indirectly measures distance along the cross-section contour; both s and t have as domain the unit interval $[0,1]$. This development is similar to that of Ballard and Brown [1].

A Generalized Cylinder is specified by a three-tuple (A, E, α). A is the *axis*, which is a curve in space defined in parametric form by $A(s) = (x_A, y_A, z_A)(s)$.

The remainder of this discussion will desribe features of the shape relative to the axis itself rather than in absolute x-y-z coordinates.

At each point $A(s)$ on the axis, let the cross-section be described on a u-v plane, with $A(s)$ at the

origin, and defined by the (constant) angle α. The u-axis will be the direction of steepest descent of the u-v plane from the tangent to the axis. α, the *angle of inclination*, is the angle from the u-axis to the tangent to the axis at $A(s)$; $\alpha = 0$ means that the u-axis is pointing towards $A(1)$, and $\alpha = \pi$ means that the u-axis is pointing towards $A(0)$.

On each u-v plane, the cross-section contour is defined by the *envelope function* $E(s,t) = (u_E, v_E)$ (s,t). On the u-v cross-section plane for each value of s, the cross-section contour is the set of points $E(s,t)$ for values of t from 0 to 1, inclusive. The contour is normally expected to be *closed*, i.e. $E(s,0) = E(s,1)$. The union of the contours is the Generalized Cylinder.

According to this strict definition, some very peculiar shapes are admitted in GC, including those with intersecting contours on different cross sections, those with singular points or arcs, and those with cross-section contours which are open arcs, points, or even space-filling curves. Since our ultimate goal is the analysis of the shapes of common objects. we will generally exclude such bizarre cases from further consideration. However, since shapes with degenerate cross-sections (open arcs or points) do have several important properties, we will note them when appropriate.

The class GC includes very many shapes: all for which there exists a space curve (axis) such that each cross-section of the object on some set of planes can be defined by a single connected component. Binford [2] defines "generalized cylinder" to be a superset of GC, allowing rotational sweeps and non-planar cross-sections. Since this definition includes such strange shapes as those described above, it is likely that some assumptions of normalcy were intended, though not explicitly stated, by Binford. Nevatia [13] has defined "generalized cones" to be GC, with the condition that α be equal to $\pi/2$, i.e. the cross-section planes are orthogonal to the axis.

2.2 Straight Generalized Cylinders

Interesting subclasses of GC arise from imposing suitable restrictions on the various component functions. The most important of these is the set of *Straight Generalized Cylinders (SGC)*, in which the axis A is linear (figure 5). The axis is thus a line segment, and all u-v planes are parallel.

This class is important because all tangents to $A(s)$ are parallel, as are all u-axes and all v-axes. We can therefore define vectors S, U, and V pointing in these directions, and assign a local (object-centered) coordinate system using u-v-s coordinates. Such coordinates can of course be defined for all Generalized Cylinders; however, there will be no curvature in the coordinate axes for SGCs. The local coordinates of an SGC are a linear transformation of world (x-y-z) coordinates. .
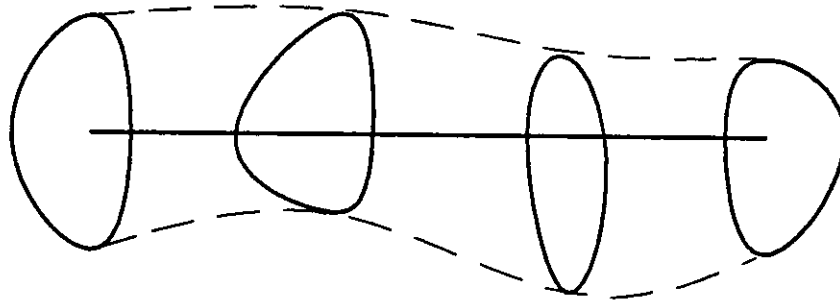
Figure 5: Straight Generalized Cylinder

2.3 Straight Homogeneous Generalized Cylinders

r(s)

t

s →

C(t)
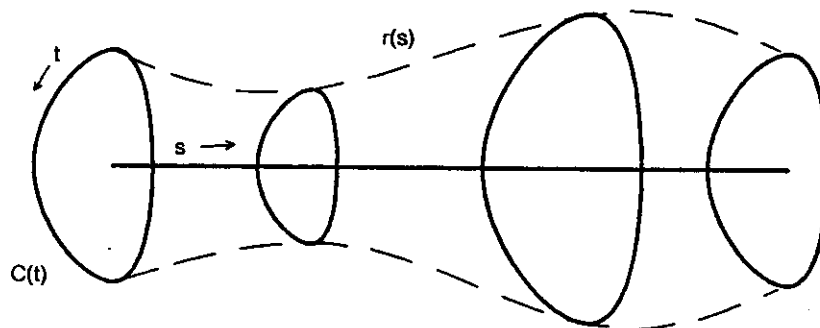
Figure 6: Straight Homogeneous Generalized Cylinder

We define a *Straight Homogeneous Generalized Cylinder (SHGC)* (figure 6) to be an SGC in which the envelope E can be decomposed into two functions by $E(s,t) = r(s)C(t)$. The *contour function* $C(t)$ = (u_c, v_c) (t) describes the *shape* of the cross-section; the radius function $r(s)$ describes its *size*. So, the cross-section has a constant shape but may vary in size. An SHGC is specified by a four-tuple (A, C, r, α).

We impose the restriction that the functions A and r be continuous and differentiable everywhere, and that the contour C be continuous and differentiable almost everywhere. It is usual, but not required, that the u-v origin be in the interior of the contour. In addition, we will presume "uniform scaling" of s and t, i.e. $\|dA/ds\|$ and $\|dC/dt\|$ are constants.

This definition of generalized cylinder is essentially the same as Marr's "generalized cone" [11].

The bulk of this paper describes the properties of SHGCs.

2.4 Subclasses of SHGC

Additional restrictions on the various functions give rise to several subclasses of SHGC with particular interesting properties:
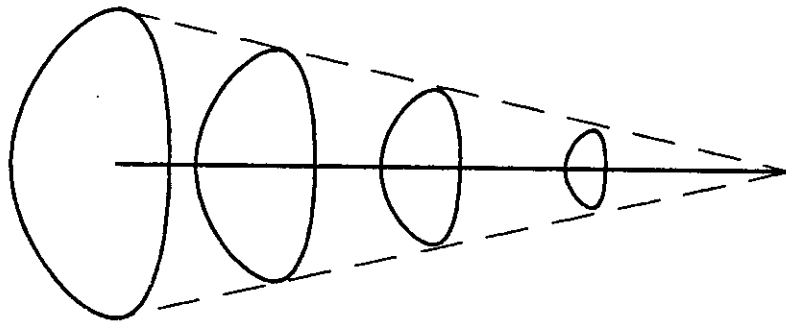
Figure 7: Linear SHGC
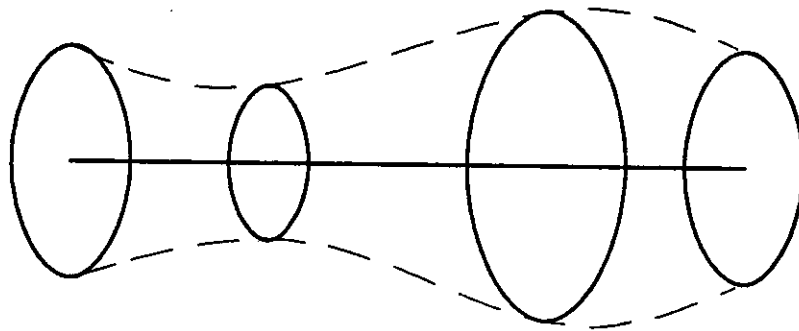
Figure 8: Circular SHGC

Linear SHGC (LSHGC) -- SHGC with r linear (figure 7)

The size of the contour varies linearly with distance along the axis. $r(s)$ can be written as $r(s) = m(s - s_0)$ for some values of m and s_0. Important relations for LSHGCs: $r(s_0) = 0$ and $dr/ds = m$. In the special case that r is constant, $r(s) = r_0$ for some value r_0. In this case, $dr/ds = 0$. LSHGCs are *ruled surfaces* as well as being Generalized Cylinders [5].
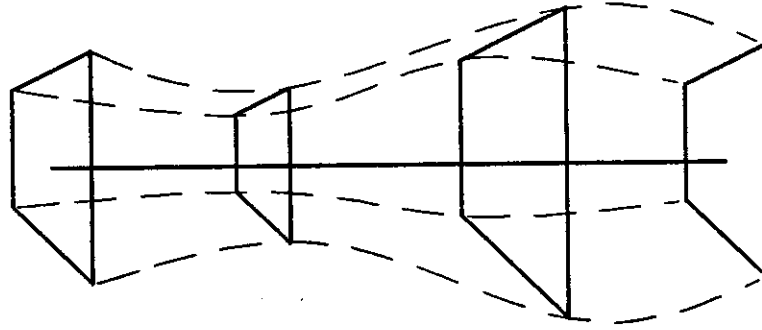
Figure 9: Polygonal SHGC

Right SHGC (RSHGC) -- SHGC with $\alpha = \pi/2$

The u-v planes are normal to the axis. There is no "direction of steepest descent" relative to the axis, so the u-axis may be chosen in any direction on the cross-section planes.

Circular SHGC (CSHGC) -- SHGC with C a circle centered at the origin (figure 8)

Without loss of generality, let C be a unit circle, $C(t) = (u_C, v_C)(t) = (\cos 2\pi t, \sin 2\pi t)$. All surfaces of solids of revolution are Right Circular SHGCs (but with open ends unless $r(0) = 0$ or $r(1) = 0$).

Polygonal SHGC (PSHGC) -- SHGC with C polygonal (piecewise linear) (figure 9)

If $C(t_0)$ is a vertex for some t_0, then the set of points $P(s,t_0)$ is a *crease* (ridge if C convex there, valley if concave). Otherwise, $P(s,t)$ is on a *face*; note that faces are not necessarily planar in this definition. On a face, $C(t)$ is linear, so it can be expressed as:

$$C(t) = (u_C(t), v_C(t)) = (m_u t + b_u, m_v t + b_v)$$

for some m_u, b_u, m_v, and b_v. If the corresponding segment of C is bounded by vertices $C(t_1) = (u_1, v_1)$ and $C(t_2) = (u_2, v_2)$, then

$$m_u = \frac{u_2 - u_1}{t_2 - t_1} \quad \text{and} \quad b_u = \frac{t_1 u_2 - t_2 u_1}{t_1 - t_2}$$

with similar definitions for m_v and b_v. In addition, $dC/dt = (du_C/dt, dv_C/dt) = (m_u, m_v)$. By the uniform scaling assumptions, t measures distance around the polygon.

In various situations, the consequences of these properties will be shown to be of special interest.

3. Fundamental Theorems and Problems

In this section, the formulae for the coordinates of a point and the direction of a surface normal for an SHGC are presented. These give rise to some important problems which are explored, and several relevant theorems are presented. These formulae and theorems provide the basis for the imaging discussion in the next section.

3.1 Coordinates for SHGCs

For any SHGC, there is a natural u-v-s object-centered coordinate system imposed by the preceding definitions. We will adopt the convention that the v-axis is chosen to provide a right-handed u-v-s coordinate system. The unit vectors in the axis directions will be denoted U, V, and S, as shown in figure 10.
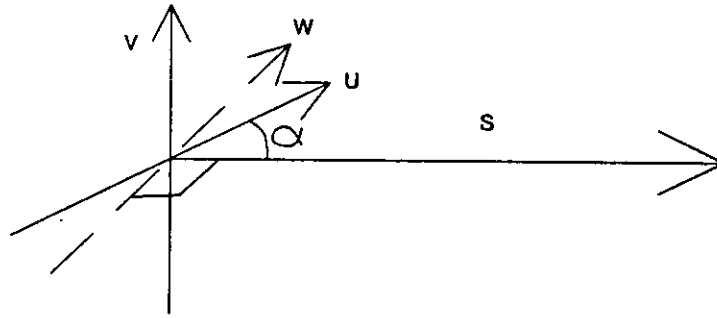
Figure 10: Coordinate Axes for SHGCs

However, $U \perp S$ only if $\alpha = \pi/2$, i.e. in a Right SHGC. Therefore, it will be convenient to define an orthogonal w-v-s coordinate system using W perpendicular to V and S. W lies in the U-S plane, with an angle of $\pi/2 - \alpha$ between W and U. For any point $(u, v, s)_{uvs}$ (where $_{uvs}$ denotes coordinates in the u-v-s system), the corresponding coordinates in w-v-s are $(u \sin \alpha, v, s + u \cos \alpha)_{wvs}$. The w-v-s coordinates are important since the axes are independent of the components of any particular Generalized Cylinder. In an RSHGC, u-v-s and w-v-s coordinates are identical.

Except where otherwise stated, all coordinates in this paper will be given in the w-v-s system.

3.1.1 Points on the Surface
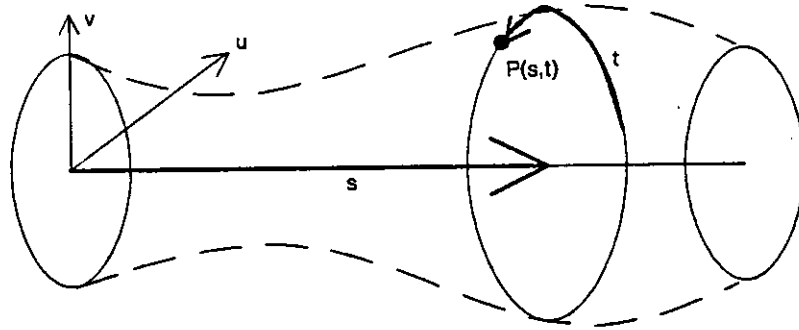
Figure 11: Coordinates of a Point on an SHGC

For any values s and t, the point $P(s, t)$ on the surface of the SHGC has u-v-s coordinates (figure 11)

$$P(s,t) = (u_C(t)\, r(s),\ v_C(t)\, r(s),\ s)_{uvs}$$

and hence w-v-s coordinates

$$P(s,t) = (u_C(t)\, r(s)\, \sin \alpha,\ v_C(t)\, r(s),\ s + u_C(t)\, r(s)\, \cos \alpha) \tag{3-1}$$

3.2 Descriptions and Shapes

A subtle problem arises from our definition of SHGCs (and other shape classes): as we have defined them, an SHGC is actually a *description of a shape* rather than being a specific solid shape itself. Of course, each such description describes a unique shape; however, we must attempt to decide when a single shape may have several different descriptions. Since a solid shape corresponds to an equivalence class of descriptions (i.e. SHGCs), we will call two descriptions *equivalent* when they describe the same solid shape, as did Marr and Nishihara in [12].

There are four trivial changes possible in the s and t coordinates themselves while preserving equivalence:

- the axis can be flipped end-over-end to yield a new SHGC (reversing the sense of the s coordinate)

- the sense of t can be likewise reversed, and, if the contour $C(t)$ is closed, the point at which $t = 0$ can be shifted to anywhere on the curve

- the radius function $r(s)$ can be multiplied by any constant scale factor, while the cross-section contour $C(t)$ is divided by the same factor

● an RSHGC can have the *u-v* axes rotated about the origin arbitrarily (shifting the *t* coordinate).

These transformations are sufficiently simple that no deeper discussion is needed.

There are, however, more significant variations in the possible descriptions of a specific shape as an SHGC. We will investigate two of the principal types of variation: altering the orientation of the cross-section planes, and altering the direction of the axis.

3.3 The Equivalent Right SHGC Problem
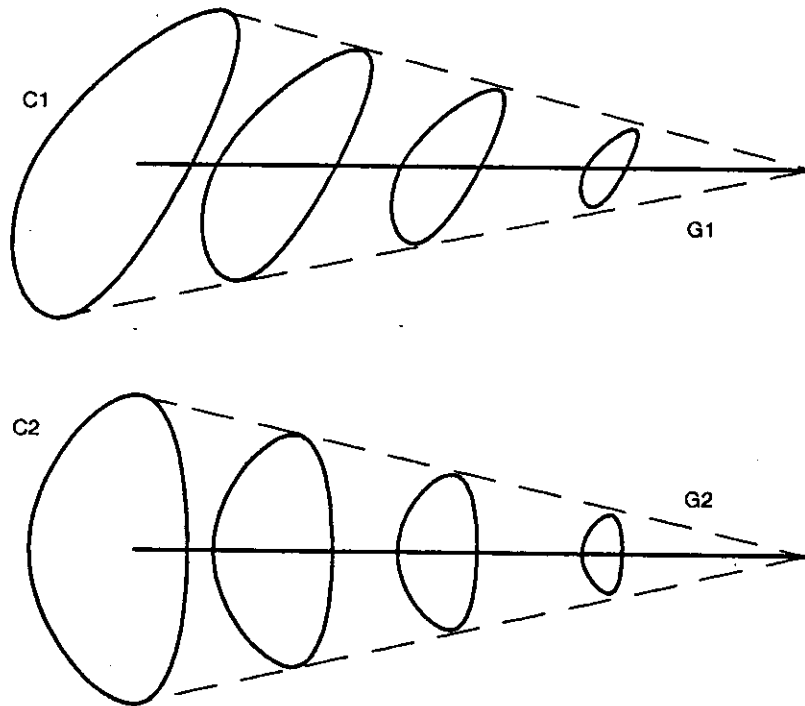
Figure 12: The Equivalent Right SHGC Problem

In figure 12, we see a shape described as two different SHGCs, with cross-section planes at different orientations. What properties of the shape make this possible? Since this question is so general, we will limit our attention to a more restricted (but still difficult) question: For what SHGCs are there equivalent Right SHGCs? This is interesting since the RSHGC seems to be a natural "canonical" form of representation for a shape. We will ignore the effect of "beveled" ends resulting from values of α not equal to $\pi/2$.

To make this problem somewhat more tractable, we will presume that the same axis A and radius function r are to be used for the SHGC and RSHGC. (We conjecture, but have not proven, that this presumption implies no loss of generality.) The problem can then be stated this way: Given an SHGC $G_1 = (A, C_1, r, \alpha)$, with $C_1 = (u_1, v_1)$, can some function $C_2 = (u_2, v_2)$ be found such that the RSHGC $G_2 = (A, C_2, r, \pi/2)$ contains the same points as G_1?

Now for each s_1 and t_1, we must have

$$P_1(s_1, t_1) = (u_1(t_1)\, r(s_1)\, \sin \alpha,\ v_1(t_1)\, r(s_1),\ s_1 + u_1(t_1)\, r(s_1)\, \cos \alpha)$$

$$= P_2(s_2, t_1) = (u_2(t_1)\, r(s_2),\ v_2(t_1)\, r(s_2),\ s_2)$$

for some s_2, with P_1 on G_1, P_2 on G_2, and with $C_2(t_1)$ corresponding to $C_1(t_1)$ for all t_1.

Equating s-coordinates,

$$s_2 = s_1 + u_1(t_1)\, r(s_1)\, \cos \alpha$$

Equating v-coordinates,

$$v_1(t_1)\, r(s_1) = v_2(t_1)\, r(s_2)$$

so

$$\frac{v_1(t_1)}{v_2(t_1)} = \frac{r(s_2)}{r(s_1)} = \frac{r(s_1 + u_1(t_1)\, r(s_1)\, \cos \alpha)}{r(s_1)}$$

Now, since

$$0 = \frac{\partial}{\partial s} \frac{v_1(t_1)}{v_2(t_1)}$$

we must have

$$0 = \frac{\partial}{\partial s} \frac{r(s_1 + u_1(t_1)\, r(s_1)\, \cos \alpha)}{r(s_1)}$$

i.e. the ratio between $r(s_2)$ and $r(s_1)$ is independent of s. So,

$$0 = \frac{1}{r(s_1)^2} \left(r(s_1) \frac{\partial}{\partial s} r(s_1 + u_1(t_1)\, r(s_1)\, \cos \alpha) - r(s_1 + u_1(t_1)\, r(s_1)\, \cos \alpha) \frac{dr}{ds}\Big|_{s1} \right)$$

$$= r(s_1) \frac{dr}{ds}\Big|_{s2} \left(1 + u_1(t_1) \cos \alpha \frac{dr}{ds}\Big|_{s1} \right) - r(s_1 + u_1(t_1)\, r(s_1)\, \cos \alpha) \frac{dr}{ds}\Big|_{s1}$$

We can differentiate this by t, using the fact that

$$\frac{\partial}{\partial t} \frac{dr}{ds}\Big|_{s2} = \frac{\partial}{\partial t} \frac{dr}{ds}\Big|_{s1 + u1(t1)r(s1)\cos\alpha}$$

$$= r(s_1)\cos\alpha \frac{du_1}{dt}\Big|_{t1} \frac{d^2r}{ds^2}\Big|_{s1 + u1(t1)r(s1)\cos\alpha} = r(s_1)\cos\alpha \frac{du_1}{dt}\Big|_{t1} \frac{d^2r}{ds^2}\Big|_{s2}$$

to obtain the condition:

$$0 = r(s_1)^2 \cos\alpha \frac{du_1}{dt}\Big|_{t1} \frac{d^2r}{ds^2}\Big|_{s2} + r(s_1)\cos\alpha \frac{dr}{ds}\Big|_{s1} \frac{\partial}{\partial t}\left(u_1(t_1)\frac{dr}{ds}\Big|_{s2}\right)$$

$$- r(s_1)\cos\alpha \frac{du_1}{dt}\Big|_{t1} \frac{dr}{ds}\Big|_{s1} \frac{dr}{ds}\Big|_{s2}$$

$$= r(s_1)^2 \cos\alpha \frac{du_1}{dt}\Big|_{t1} \frac{d^2r}{ds^2}\Big|_{s2} + r(s_1)^2 u_1(t_1)\cos\alpha \frac{du_1}{dt}\Big|_{t1} \frac{dr}{ds}\Big|_{s1} \frac{d^2r}{ds^2}\Big|_{s2}$$

$$= r(s_1)^2 \cos\alpha \frac{du_1}{dt}\Big|_{t1} \frac{d^2r}{ds^2}\Big|_{s2}\left(1 + u_1(t_1)\frac{dr}{ds}\Big|_{s1}\right)$$

So, one of the above terms must be 0. If $r(s) = 0$, G_1 is degenerate (cross-section is a single point). If $\cos\alpha = 0$, G_1 is already a Right SHGC. If $du_1/dt = 0$, G_1 is degenerate ($C(t)$ is a line of constant u). If $0 = d^2r/ds^2$, G_1 is a Linear SHGC. And finally, if $0 = 1 + u_1(t)\,dr/ds$, we can differentiate by s to yield $0 = u_1(t)\,d^2r/ds^2$ and G_1 is either degenerate ($0 = u_1(t)$) or Linear ($0 = d^2r/ds^2$).

So, if an SHGC G_1 has an equivalent representation as an RSHGC, then either (1) G_1 is degenerate, (2) G_1 is an LSHGC, or (3) G_1 is already an RSHGC.

3.3.1 The Slant Theorem

The Equivalent RSHGC Problem suggests that the only nondegenerate SHGCs with equivalent representation as RSHGCs are LSHGCs. The converse is also true: Every Linear SHGC has an equivalent representation that is also an RSHGC. In other words, the set of all LSHGCs is a subset of all RSHGCs.

This statement is called the *Slant Theorem*, which says in effect that it doesn't matter what direction the cross-section planes are taken relative to the axis of an LSHGC: for any direction, some contour function C can be found to describe the shape (ignoring the possible beveling of the ends) (figure 13).

To prove the theorem, let $G_1 = (A, C_1, r, \alpha)$ be an LSHGC with $r = m(s - s_0)$ and $C_1 = (u_1, v_1)$. (We will deal with the special case $r(s) = r_0$ below.) The constituent points are

$$P_1(s_1, t_1) = (u_1(t_1)\,m\,(s_1 - s_0)\sin\alpha,\ v_1(t_1)\,m\,(s_1 - s_0),\ s_1 + u_1(t_1)\,m\,(s_1 - s_0)\cos\alpha)$$
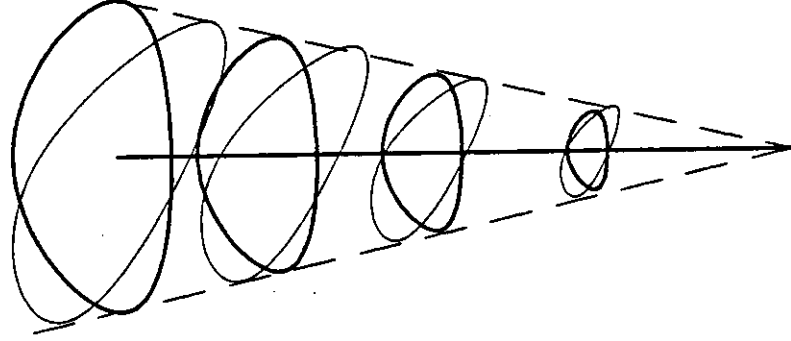
Figure 13: The Slant Theorem

Now consider $G_2 = (A, C_2, r, \pi/2)$, which is an LSHGC and RSHGC with A and r as above, and C_2 = (u_2, v_2). Let u_2 and v_2 be defined by:

$$u_2(t) = \frac{u_1(t)\, \sin\alpha}{1 + u_1(t)\, m\, \cos\alpha}$$

$$v_2(t) = \frac{v_1(t)}{1 + u_1(t)\, m\, \cos\alpha}$$

(This definition violates the uniform scaling assumption for t; however, the contour can be deformed along its length to eliminate this problem, and in any event this condition is not central to the derivation being presented.) Each point of G_2 has coordinates

$$P_2(s_2, t_2) = (u_2(t_2)\, r(s_2),\ v_2(t_2)\, r(s_2),\ s_2)$$

$$= \left(\frac{u_1(t_2)\, m\, (s_2 - s_0)\, \sin\alpha}{1 + u_1(t_2)\, m\, \cos\alpha},\ \frac{v_1(t_2)\, m\, (s_2 - s_0)}{1 + u_1(t_2)\, m\, \cos\alpha},\ s_2 \right)$$

Now, for each s_1 and t_1, define s_2 and t_2 by:

$$s_2 = s_1 + u_1(t_1)\, m\, (s_1 - s_0)\, \cos\alpha$$
$$t_2 = t_1$$

Then

$$P_2(s_2, t_2) = \left(\frac{u_1(t_1)\, m\, (s_1 + u_1(t_1)\, m\, (s_1 - s_0)\, \cos\alpha - s_0)\, \sin\alpha}{1 + u_1(t_1)\, m\, \cos\alpha}, \right.$$

$$\frac{v_1(t_1)\, m\, (s_1 + u_1(t_1)\, m\, (s_1 - s_0)\, \cos\alpha - s_0)}{1 + u_1(t_1)\, m\, \cos\alpha},$$

$$\left. s_1 + u_1(t_1)\, m\, (s_1 - s_0)\, \cos\alpha \right)$$

$$= (u_1(t_1) \, m \, (s_1 - s_0) \sin \alpha, \, v_1(t_1) \, m \, (s_1 - s_0), \, s_1 + u_1(t_1) \, m \, (s_1 - s_0) \cos \alpha)$$
$$= P_1(s_1, t_1)$$

Thus, for each s_1 and t_1, there exists a point $P_2(s_2, t_2)$ on G_2 which is the same as the point $P_1(s_1, t_1)$ on G_1, i.e. G_1 and G_2 contain the same points. The beveling of the ends of G_1 but not G_2 is reflected in the restriction that s_2 must lie in the interval $[0,1]$.

In the special case that $r(s)$ is constant, we have $r(s) = r_0$. Then

$$P_1(s_1, t_1) = (u_1(t_1) \, r_0 \sin \alpha, \, v_1(t_1) \, r_0, \, s_1 + u_1(t_1) \, r_0 \cos \alpha)$$

So let u_2 and v_2 be defined by:

$$u_2(t) = u_1(t) \sin \alpha$$
$$v_2(t) = v_1(t)$$

Then, for each s_1 and t_1, define s_2 and t_2 by:

$$s_2 = s_1 + u_1(t_1) \, r_0 \cos \alpha$$
$$t_2 = t_1$$

Then we have:

$$P_2(s_2, t_2) = (u_1(t_2) \, r_0 \sin \alpha, \, v_1(t_2) \, r_0, \, s_2)$$
$$= P_1(s_1, t_1)$$

and the above conclusions hold true for this case.

So, for each LSHGC, there exists another description of the same shape which is both an LSHGC and RSHGC, containing all the same points (but without beveled ends). In this sense, the set of LSHGCs is a subset of the set of RSHGCs.

3.4 The Alternate Axis Problem

Having explored the issue of changing the cross-section planes, we can ask about moving the axis: For what SHGCs are there equivalent representations with different axes, using the same cross-section planes (figure 14)? (This is known to involve a loss of generality with respect to the question: For what SHGCs are there equivalent representations with different axes? For example, a sphere satisfies the latter condition, but not the condition we are addressing here. We conjecture that only shapes resembling certain regular polyhedra, of which the sphere is the limiting case, are excluded from our analysis herein by the restriction to use the same cross-section planes.) We will begin by restricting the problem so that the two axes intersect somewhere, and so that both axes intersect the cross-section planes (i.e. the axes of the SHGCs are not parallel to the cross-section planes).
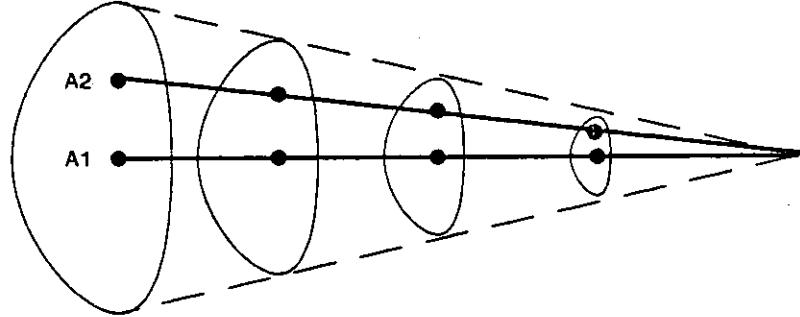
Figure 14: The Alternate Axis Problem

Suppose $G_1 = (A_1, C_1, r_1, \alpha_1)$ and $G_2 = (A_2, C_2, r_2, \alpha_2)$ are SHGCs representing the same shape, with the same u-v planes, and with $A_1(s_0) = A_2(s_0)$ for some s_0. (We will presume the u-axis is oriented identically for G_1 and G_2, without loss of generality since the u-v axes could be rotated without affecting the following line of reasoning. Similarly, the exact definition of α_2 is not of interest here -- it is sufficient to note that it is in fact constant since A_2 is a line segment and all u-v planes are parallel.)

Let $A_2(s_0 + 1) = (u_{A2}, v_{A2})_{u1v1}$, i.e. (u_{A2}, v_{A2}) are the coordinates in the u-v plane for G_1 of the origin of the u-v plane for G_2, for the value $s = s_0 + 1$. Then for any s,

$$A_2(s) = (0, 0)_{u2v2}$$
$$= (u_{A2} (s - s_0), v_{A2} (s - s_0))_{u1v1}$$

since the axes A_1 and A_2 are linear.

For any point $P(s,t)$ on G_1,

$$P(s,t) = (u_1(t) r_1(s), v_1(t) r_1(s), s)_{u1v1s}$$
$$= (u_1(t) r_1(s) - u_{A2} (s - s_0), v_1(t) r_1(s) - v_{A2} (s - s_0), s)_{u2v2s}$$

since the origin is translated by $(u_{A2} (s - s_0), v_{A2} (s - s_0))$. But since $P(s,t)$ must also be a point on G_2,

$$P(s,t) = (u_2(t) r_2(s), v_2(t) r(s), s)_{u2v2s}$$

Equating u-coordinates,

$$u_1(t) r_1(s) - u_{A2} (s - s_0) = u_2(t) r_2(s)$$

Differentiating by s,

$$u_1(t) \frac{dr_1}{ds} - u_{A2} = u_2(t) \frac{dr_2}{ds}$$

and differentiating by s again,

$$u_1(t) \frac{d^2 r_1}{ds^2} = u_2(t) \frac{d^2 r_2}{ds^2}$$

$$\frac{u_1(t)}{u_2(t)} \frac{d^2 r_1}{ds^2} = \frac{d^2 r_2}{ds^2}$$

Now differentiating by t,

$$\frac{d^2 r_1}{ds^2} \frac{d}{dt} \frac{u_1(t)}{u_2(t)} = 0$$

So,

$$\frac{d^2 r_1}{ds^2} = 0 \quad \text{or} \quad \frac{d}{dt} \frac{u_1(t)}{u_2(t)} = 0$$

If $d^2 r_1/ds^2 = 0$, G_1 is an LSHGC.

Suppose $d^2 r_1/ds^2 \neq 0$. Then $d/dt \, u_1(t)/u_2(t) = 0$, and $u_2(t) = k \, u_1(t)$ for some constant k. But, we already know that

$$u_2(t) \, r_2(s) = u_1(t) \, r_1(s) - u_{A2} (s - s_0)$$

so

$$u_1(t) = \frac{u_{A2} (s - s_0)}{r_1(s) - k \, r_2(s)}$$

Differentiating by t, we have

$$\frac{du_1}{dt} = 0$$

so $u_1(t) = u_0$ for some constant u_0. By similarly equating v-coordinates, we have $v_1(t) = v_0$ for some constant v_0, i.e. the cross-section is a single point, and G_1 is thus a degenerate Generalized Cylinder.

Thus, a nondegenerate shape can be represented as SHGCs with different (intersecting) axes only if the shape is an LSHGC.

3.4.1 The Pivot Theorem
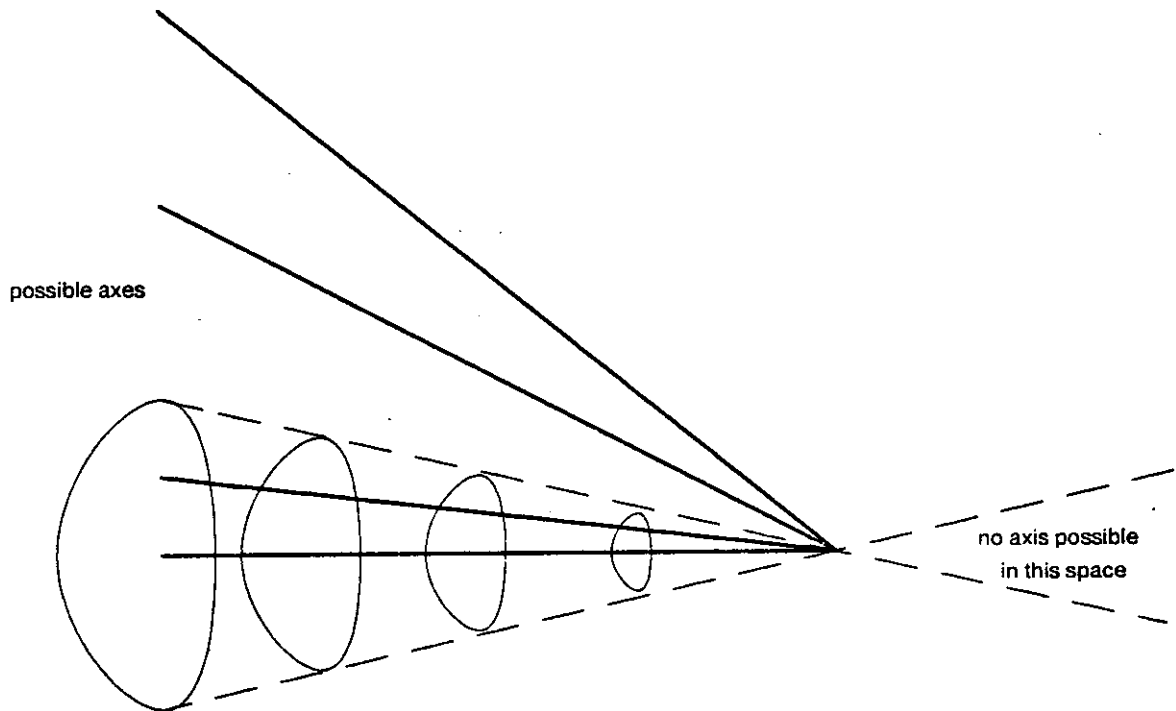
Figure 15: The Pivot Theorem

The alternate axis problem suggests that the only SHGCs with equivalent representations with different axes are LSHGCs. The converse is also true: each LSHGC can be represented with the axis pointing in any direction, so long as it contains the *apex* point of the shape (the point at which its radius is 0) (figure 15). (We will observe a minor restriction on the direction of the axis later in this section). This statement is called the *Pivot Theorem* since it states that the axis of an LSHGC can effectively be pivoted about the apex into any direction.

To prove the theorem, let $G_1 = (A_1, C_1, r, \alpha_1)$ and $G_2 = (A_2, C_2, r, \alpha_2)$ be LGCs describing the same shape, with $r(s) = m\ (s - s_0)$, with the same u-v planes (possibly rotated as in the previous section), and with $A_1(s_0) = A_2(s_0)$. ($A_1(s_0)$ is the apex of the shape, since $r(s_0) = 0$.)

Let the u-v coordinates of $A_2(s_0 + 1)$ on the u-v plane for G_1 be $(u_{A2}, v_{A2})_{u1v1}$. Then for all s,

$$A_2(s) = (u_{A2}\ (s - s_0),\ v_{A2}\ (s - s_0))_{u1v1}$$

since the axes are both linear.

Now, let $C_1 = (u_1, v_1)$ and $C_2 = (u_2, v_2)$ where:

$$u_2(t) = u_1(t) - \frac{u_{A2}}{m} \quad \text{and} \quad v_2(t) = v_1(t) - \frac{v_{A2}}{m}$$

For any point $P(s,t)$ on G_1,

$$
\begin{aligned}
P(s,t) &= (u_1(t)\,r(s),\ v_1(t)\,r(s),\ s)_{u1v1s} \\
&= (u_1(t)\,r(s) - u_{A2}(s - s_0),\ v_1(t)\,r(s) - v_{A2}(s - s_0),\ s)_{u2v2s} \\
&= (u_1(t)\,m\,(s - s_0) - u_{A2}(s - s_0),\ v_1(t)\,m\,(s - s_0) - v_{A2}(s - s_0),\ s)_{u2v2s} \\
&= \left(\left[u_1(t) - \frac{u_{A2}}{m}\right]m\,(s - s_0),\ \left[v_1(t) - \frac{v_{A2}}{m}\right]m\,(s - s_0),\ s \right)_{u2v2s} \\
&= (u_2(t)\,r(s),\ v_2(t)\,r(s),\ s)_{u2v2s}
\end{aligned}
$$

which is a point on G_2. So, each point of G_1 is also a point of G_2 (and vice versa, by similar reasoning). Thus, G_1 and G_2 describe the same shape.

By two applications of the Slant Theorem, we can eliminate the requirement that A_2 pass through the u-v planes of G_1. So, for any LSHGC, the axis may be defined in any direction, but must pass through the apex.

Two additional restrictions must be noted: the shape may be beveled differently in the two representations just as in the Equivalent RSHGC Problem; and, the u-v planes must pass completely through the shape, so the axis is actually prevented from pointing directly away from the shape. This latter restriction excludes the axis from belonging to the projection of the shape through its own apex (figure 15).

3.5 Surface Normals of an SHGC

The surface normals for an SHGC can be defined wherever the contour function $C(t)$ is differentiable (figure 16).

Equation (3-1) gave the coordinates of a point $P(s,t)$ on an SHGC. From this, we can calculate the tangent vector to the surface in the direction of increasing s as

$$\frac{\partial P}{\partial s} = \left(u_C(t)\,\sin\alpha\,\frac{dr}{ds},\ v_C(t)\,\frac{dr}{ds},\ 1 + u_C(t)\,\cos\alpha\,\frac{dr}{ds} \right)$$

and the tangent in the direction of increasing t as
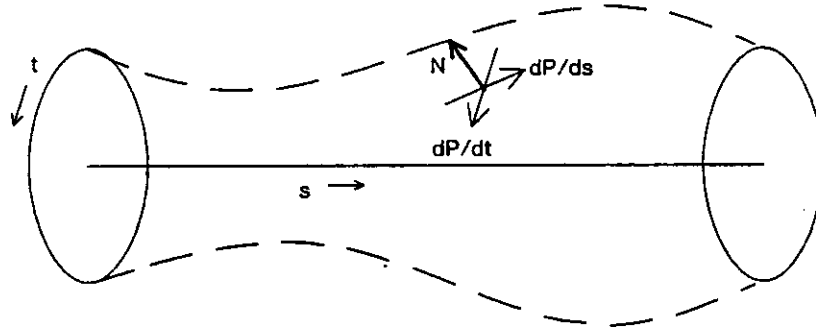
Figure 16: Surface Normal of an SHGC

$$\frac{\partial P}{\partial t} = \left(r(s)\, sin.\, \alpha\, \frac{du_C}{dt},\ r(s)\, \frac{dv_C}{dt},\ r(s)\, cos\, \alpha\, \frac{du_C}{dt} \right)$$

$$= r(s) \left(sin\, \alpha\, \frac{du_C}{dt},\ \frac{dv_C}{dt},\ cos\, \alpha\, \frac{du_C}{dt} \right)$$

So, the outward-pointing surface normal vector $N'(s,t)$ at $P(s,t)$ is the cross product of these:

$$N'(s,t) = \frac{\partial P}{\partial t} \times \frac{\partial P}{\partial s}$$

$$= r(s) \left(-v_C(t)\, cos\, \alpha\, \frac{dr}{ds}\, \frac{du_C}{dt} + \frac{dv_C}{dt} + u_C(t)\, cos\, \alpha\, \frac{dr}{ds}\, \frac{dv_C}{dt}, \right.$$

$$- sin\, \alpha\, \frac{du_C}{dt},$$

$$\left. - u_C(t)\, sin\, \alpha\, \frac{dr}{ds}\, \frac{dv_C}{dt} + v_C(t)\, sin\, \alpha\, \frac{dr}{ds}\, \frac{du_C}{dt} \right)$$

$$= r(s) \left(h(t)\, cos\, \alpha\, \frac{dr}{ds} + \frac{dv_C}{dt},\ - sin\, \alpha\, \frac{du_C}{dt},\ - h(t)\, sin\, \alpha\, \frac{dr}{ds} \right)$$

where $h(t)$, defined by

$$h(t) = u_C(t)\, \frac{dv_C}{dt} - v_C(t)\, \frac{du_C}{dt} = \begin{vmatrix} u_C & v_C \\ du_C/dt & dv_C/dt \end{vmatrix}$$

is the *Wronskian* of the contour functions u_C and v_C [14]; $h(t) = 0$ implies that the SHGC has a line segment for a cross-section contour, i.e. is degenerate.

We will use $N(s,t)$ parallel to $N'(s,t)$, defined by

$$N(s,t) = \frac{N'(s,t)}{r(s)} = \left(h(t) \cos \alpha \frac{dr}{ds} + \frac{dv_C}{dt}, \ -\sin \alpha \frac{du_C}{dt}, \ -h(t) \sin \alpha \frac{dr}{ds} \right)$$

3.6 The Corresponding Normal Theorem
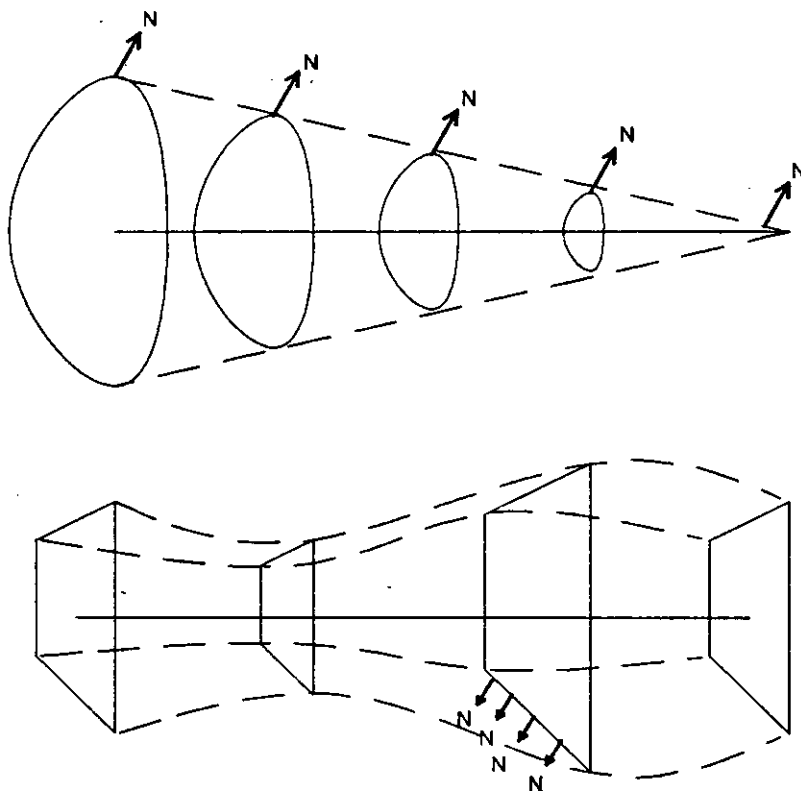
Figure 17: The Corresponding Normal Theorem

Figure 17 shows that the surface normals on a Linear SHGC are parallel along contours of constant t, and for a Polygonal SHGC they are parallel along contours of constant s within a face. This is stated in the *Corresponding Normal Theorem*: An SHGC is Linear iff for all s, $\partial N/\partial s = (0,0,0)$; an SHGC is Polygonal iff for almost all t, $\partial N/\partial t = (0,0,0)$. This says that the surface normals for an LSHGC depend only on t, and for a face of a PSHGC depend only on s.

For the first part of the theorem, we begin by noting that

$$\frac{\partial N}{\partial s} = \left(h(t) \cos \alpha \frac{d^2 r}{ds^2}, \ 0, \ -h(t) \sin \alpha \frac{d^2 r}{ds^2} \right)$$

Now for an LSHGC, $d^2r/ds^2 = 0$, so $\partial N/\partial s = (0,0,0)$ for all s.

Conversely, if $\partial N/\partial s = (0,0,0)$ for all s, then either $h(t) = 0$, $sin\ \alpha$ and $cos\ \alpha$ are both 0, or $d^2r/ds^2 = 0$. If $h(t) = 0$, the shape is degenerate. It is impossible for $sin\ \alpha$ and $cos\ \alpha$ to both be 0. So, the only interesting case is that in which $d^2r/ds^2 = 0$, i.e. the shape is an LSHGC.

For the second part of the theorem, note that

$$\frac{\partial N}{\partial t} = \left(cos\ \alpha\ \frac{dr}{ds}\ \frac{dh}{dt} + \frac{d^2v_C}{dt^2}, \quad -sin\ \alpha\ \frac{d^2u}{dt^2}, \quad -sin\ \alpha\ \frac{dr}{ds}\ \frac{dh}{dt} \right)$$

where

$$\frac{dh}{dt} = u_C(t)\ \frac{d^2v_C}{dt^2} - v_C(t)\ \frac{d^2u_C}{dt^2}$$

Now for a PSHGC, $d^2u_C/dt^2 = 0$ and $d^2v_C/dt^2 = 0$ for almost all t (except at the vertices), so $dh/dt = 0$ and $\partial N/\partial t = (0,0,0)$.

Conversely, suppose $\partial N/\partial t = (0,0,0)$ almost everywhere. Using the v-coordinate, since $sin\ \alpha = 0$ is impossible (it implies that $\alpha = 0$, i.e. the axis is contained in the cross-section planes), it must be that $d^2u_C/dt^2 = 0$. Then wherever $\partial N/\partial t = (0,0,0)$, we have

$$\frac{\partial N}{\partial t} = \left((1 + u_C(t)\ cos\ \alpha\ \frac{dr}{ds})\ \frac{d^2v_C}{dt^2}, \quad 0, \quad -u_C(t)\ sin\ \alpha\ \frac{dr}{ds}\ \frac{d^2v_C}{dt^2} \right)$$

So from the s-coordinate, either $u_C(t) = 0$ or $dr/ds = 0$ or $d^2v_C/dt^2 = 0$. If $u_C(t) = 0$, the SHGC is degenerate (planar). If $dr/ds = 0$, using the u-coordinate, $d^2v_C/dt^2 = 0$. So, the only interesting case is that in which $d^2u_C/dt^2 = 0$ and $d^2v_C/dt^2 = 0$, i.e. the contour $C(t)$ is locally linear. When this is true for almost all t, $C(t)$ is piecewise linear and the shape must be a Polygonal SHGC.

The Corresponding Normal Theorem is especially useful in shadow geometry, since the "shadow volume" (the volume of space shaded by an object) is an LSHGC (figure 18) [17].
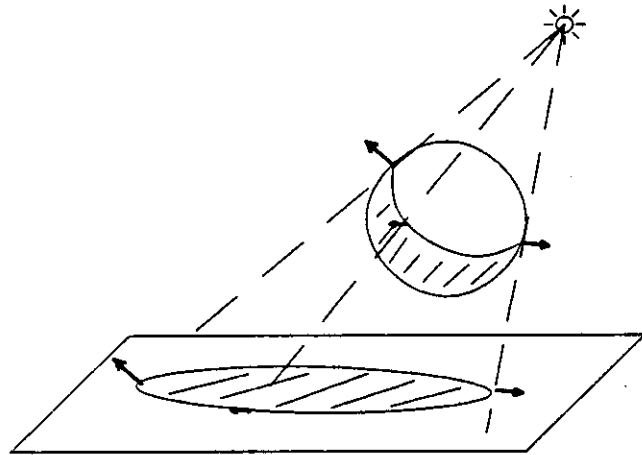
Figure 18: Surface Normals of the Shadow Volume

4. Projections of SHGCs

In this section, we will begin by exploring the projections of SHGCs onto images. Then, we will describe how images can be analyzed to determine the SHGCs depicted. Although the formulations will begin with the most general cases, most of our attention will be given to the case of Right Circular SHGCs, since these are sufficiently constrained to allow interesting analysis from imagery without additional knowledge sources.

4.1 Projected Contour Generators
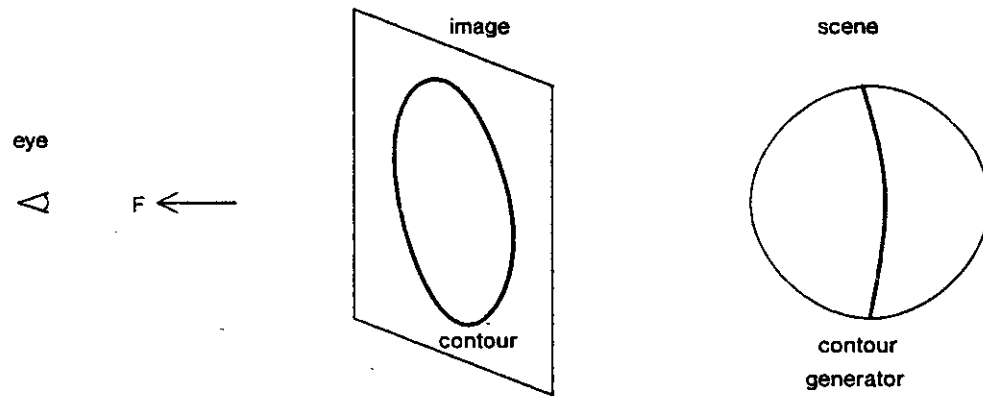
Figure 19: Contours and Contour Generators

Suppose we have an SHGC, and we project it along the direction of a vector $F = (f_w, f_v, f_s)$, as in figure 19. The contours along which the surface is tangent to the line of sight as seen from direction F (i.e. occlusion, or parallelism to F) will be projected by the ends of the SHGC, or where $N \perp F$, i.e. $N \cdot F = 0$. The points on the SHGC projected onto such contours are called *contour generators* [11]. (Of course, if the SHGC is opaque, some of the contours may be hidden from view.) From this point on, we will use the term "contour" to mean "image of a contour generator" (in the above sense), and "cross-section function" to refer to $C(t)$.

On the contour generators,

$$0 = N \cdot F = f_w \left(h(t) \cos \alpha \frac{dr}{ds} + \frac{dv_C}{dt} \right) - f_v \sin \alpha \frac{du_C}{dt} - f_s h(t) \sin \alpha \frac{dr}{ds}$$

where $h(t)$ is the contour Wronskian, as previously described.
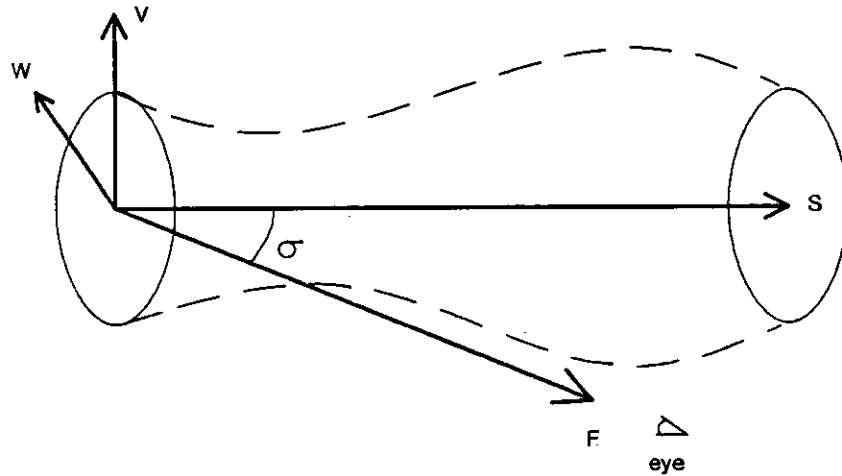
Figure 20: Viewing Direction and Angle

Unless otherwise stated, we will presume in the following discussion of projection and imaging that we are dealing only with Right SHGCs, i.e. SHGCs with cross-sections perpendicular to the axis. This allows the simplification of rotating the w-v axes as desired; in particular, we will presume that F is in the W-S plane, i.e. $f_v = 0$. Without loss of generality, we can then presume that F is between $-W$ and S; if the angle from F to S (the *viewing angle*) is σ, then $F = (-\sin \sigma, 0, \cos \sigma)$ (figure 20). Additional simplification arises for an RSHGC since $\sin \alpha = 1$ and $\cos \alpha = 0$. Then, for an RSHGC, the contour generator points satisfy

$$0 = \sin \sigma \, \frac{dv_c}{dt} + h(t) \cos \sigma \, \frac{dr}{ds} \tag{4-1}$$

There are three interesting cases, illustrated in figure 21: end, side, and oblique views. If $F \parallel S$ ("end view"), $\sin \sigma = 0$ and the contour generator points satisfy

$$0 = h(t) \frac{dr}{ds}$$

In this case, either $h(t) = 0$ or $\frac{dr}{ds} = 0$. But, $h(t) = 0$ only if the RSHGC is degenerate (planar), so the only interesting case is $dr/ds = 0$, i.e. the contour generators are cross-sections at extrema (relative maxima and minima) of $r(s)$ (Marr's "radial extremities" [11]).

If $F \parallel W$ ("side view"), $\cos \sigma = 0$ and the contour generator points satisfy
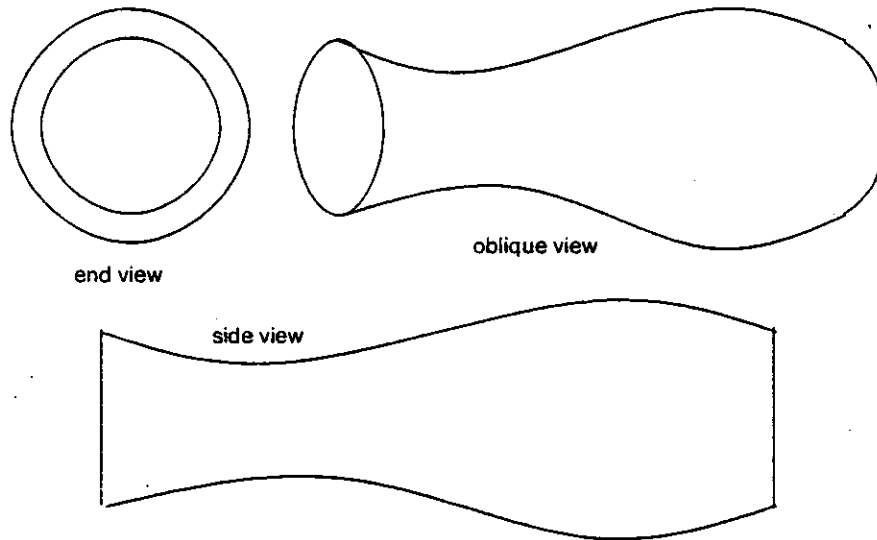
Figure 21: End, Side, and Oblique Views

$$0 = \frac{dv_{c}}{dt}$$

So, the contour generators are at the extrema of $v_{c}(t)$.

If $F \| S$ and $F \| W$ ("oblique view"), there is no simplification from equation (4-1).

It is easy to imagine a dichotomy for oblique views between "end-like" views and "side-like" views as if there were an abrupt change from one to the other as F swings from S to W. However, there is actually no abrupt change, but rather a steady change in the contour generators.

4.1.1 Planarity of Contour Generators

A set of points $\{P\} = \{(p_{w}, p_{v}, p_{s})\}$ is planar iff there exist constants a, b, c, and d such that, for all points in the set, $ap_{w} + bp_{v} + cp_{s} + d = 0$. We can use this to determine some conditions on planarity of contour generators.

In an end view, $0 = dr/ds$ along a contour generator. Thus, the points on a contour generator satisfy $p_{s} = s_{0}$ where $dr/ds \big|_{s_{0}} = 0$. So,

$$0 p_{w} + 0 p_{v} + p_{s} - s_{0} = 0$$

and the contour generator must therefore be planar. Further, the plane containing the contour generator is perpendicular to the viewing direction $F = (0, 0, 1)$ for an end view since $F \cdot P - s_{0} = 0$.

In a side view, $0 = dv_C/dt$. But this is a function of t, so $dv_C/dt \big|_{t_0} = 0$ for some t_0. Each such value of t_0 defines a single contour generator. On this contour generator, $t = t_0$ and

$$P(s,t_0) = (p_w, p_v, p_s) = (u_C(t_0) r(s), v_C(t_0) r(s), s)$$

$$p_w v_C(t_0) = p_v u_C(t_0)$$

$$v_C(t_0) p_w - u_C(t_0) p_v + 0 p_s + 0 = 0$$

so the contour generator is planar. In addition, if for such t_0 we have $u_C(t_0) = 0$, then the equation can be simplified to $p_w = 0$, i.e. the plane containing the contour generator is perpendicular to F (and parallel to the image plane).

However, for oblique views, the contour generators are generally not planar. There is no easy method for evaluating the planarity of the contour generator defined by equation (4-1). Instead of the above criterion, if specific functions $u_C(t)$, $v_C(t)$, and $r(s)$ are known, the *torsion* of the contour generator can be evaluated; it must be 0 for the contour generator to be planar [4].

In the special case of LSHGCs, we have $r = m (s - s_0)$ and $dr/ds = m$. So, the contour generator satisfies:

$$0 = \sin \sigma \frac{dv_C}{dt} + m h(t) \cos \sigma \tag{4-2}$$

The above expression is only a function of t. Thus, for a given contour generator, the above equation holds true for some value of t_0, and the contour generator is planar by the same reasoning as used for a side view. So, for an LSHGC, every contour generator is planar.

4.2 Images of Right SHGCs

The world coordinate system is defined as shown in figure 22, by aligning X and Y horizontally and vertically (respectively) on the image plane, and letting Z point towards the eye (or camera) The viewing direction F is then the same as Z, i.e. $F = (0,0,1)_{xyz}$ (where xyz denotes world coordinates). The discussion of imaging in this paper will be primarily limited to *orthographic projection*, in which a world point $(x,y,z)_{xyz}$ is mapped onto the image point $(x,y)_{xy}$.

Suppose we are looking at an RSHGC. Without loss of generality, we can presume that S is in the X-Z plane, between Z and X. Then the viewing angle σ is measured from Z towards S (since $F = Z$). Since W-V-S is right-handed, W is in the X-Z plane between X and $-Z$ and V points vertically upward, $V = Y$. The important vectors are then:
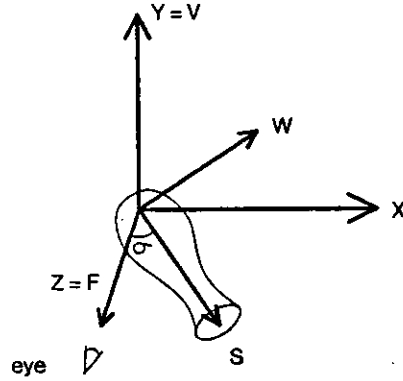
Figure 22: Object and World Coordinate Systems

$$F = (-\sin \sigma, \ 0, \ \cos \sigma)_{wvs} = (0, \ 0, \ 1)_{xyz}$$

$$W = (1, \ 0, \ 0)_{wvs} = (\cos \sigma, \ 0, \ -\sin \sigma)_{xyz}$$

$$V = (0, \ 1, \ 0)_{wvs} = (0, \ 1, \ 0)_{xyz}$$

$$S = (0, \ 0, \ 1)_{wvs} = (\sin \sigma, \ 0, \ \cos \sigma)_{xyz}$$

For any point P,

$$P = (w, v, s)_{wvs} = w\,W + v\,V + s\,S$$
$$= (w \cos \sigma + s \sin \sigma, \ v, \ -w \sin \sigma + s \cos \sigma)_{xyz}$$

A point $P(s,t)$ on an RSHGC is therefore

$$P(s,t) = (u_C(t)\,r(s), \ v_C(t)\,r(s), \ s)_{wvs}$$
$$= (u_C(t)\,r(s) \cos \sigma + s \sin \sigma, \ v_C(t)\,r(s), \ -u_C(t)\,r(s) \sin \sigma + s \cos \sigma)_{xyz}$$

and its image under orthography is (figure 23)

$$I(s,t) = (x,y)\,(s,t)_{xy} = (u_C(t)\,r(s) \cos \sigma + s \sin \sigma, \ v_C(t)\,r(s))_{xy}$$

We will presume that the image of the origin of the RSHGC is $(0,0)_{xy}$; otherwise, an additional translation of the image points will occur. In addition, we are presuming here that there is no scaling difference between w-v-s and x-y-z coordinates.

4.2.1 Contour Generators Under Perspective Projection

While the bulk of this discussion concerns orthographic projection, in which the image of a point $(x, y, z)_{xyz}$ is $(x, y)_{xy}$, it is also possible to analyze the contours of RSHGCs viewed under *perspective projection*, in which the image of $(x, y, z)_{xyz}$ is $(-x/z, \ -y/z)_{xy}$ if the unit of measure is the focal length
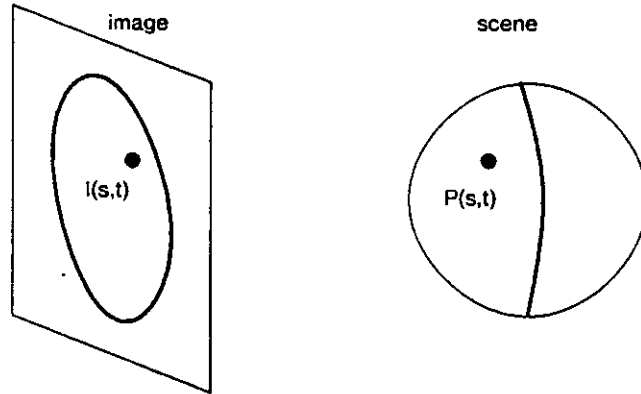
Figure 23: Image of a Point on a Right SHGC

of the lens (this is the same coordinate system as that of Shafer et al. [15]). Since translation in space affects a perspective image, it is necessary to generalize the imaging model used above to allow for the position of the object in the scene, as well as the possibility that the axis of the image of the object does not pass through the origin of the image.
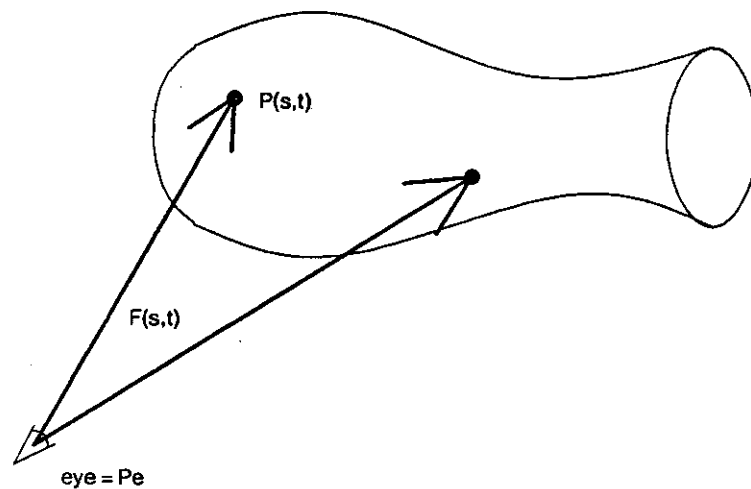
Figure 24: Imaging Under Perspective Projection

The contour generator analysis itself can be accomplished by considering the eye (center of the lens) to be located at a point $P_e = (w_e, v_e, s_e)$ in the object-centered coordinate system, as in figure 24. Then, at each point $P(s,t)$ on the surface of the object, the line of sight is the vector $F(s,t)$ from the eye to $P(s,t)$, defined by:

$$F(s,t) = P(s,t) - P_e$$

$$= (u_C(t) \, r(s) - w_e, v_C(t) \, r(s) - v_e, s - s_e)$$

Along a contour generator, we still have $N \perp F$, so $0 = N \cdot F$.

While both the imaging and contour generator problems are therefore more difficult under perspective projection, they may still be solvable, particularly for relatively constrained cases such as the analysis of Right Circular SHGCs.

4.3 Projection and Imaging for Right Circular SHGCs

For Right SHGCs which are also Circular SHGCs (CSHGCs), there is considerable simplification in the orthographic projection and imaging relationships. Recall that, for a Circular SHGC,

$$u_C(t) = \cos 2\pi t \quad \text{and} \quad v_C(t) = \sin 2\pi t$$

So,

$$\frac{du_C}{dt} = -2\pi \sin 2\pi t \quad \text{and} \quad \frac{dv_C}{dt} = 2\pi \cos 2\pi t$$

and

$$h(t) = u_C \frac{dv_C}{dt} - v_C \frac{du_C}{dt} = 2\pi \cos^2 2\pi t + 2\pi \sin^2 2\pi t$$

$$= 2\pi$$

The contour generators for an RCSHGC therefore satisfy

$$0 = 2\pi \sin \sigma \cos 2\pi t + 2\pi \cos \sigma \frac{dr}{ds}$$

i.e. (figure 25)

$$t = \frac{1}{2\pi} \cos^{-1} \left(-\cot \sigma \frac{dr}{ds} \right) \tag{4-3}$$

So along the contour generator,

$$u_C(t) = \cos 2\pi t = -\cot \sigma \frac{dr}{ds}$$

$$v_C(t) = \sin 2\pi t = \pm \sqrt{1 - u_C(t)^2} = \pm \sqrt{1 - \cot^2 \sigma \, (dr/ds)^2}$$

where $v_C(t) \geq 0$ on the upper half of the shape, and $v_C(t) \leq 0$ on the lower half.
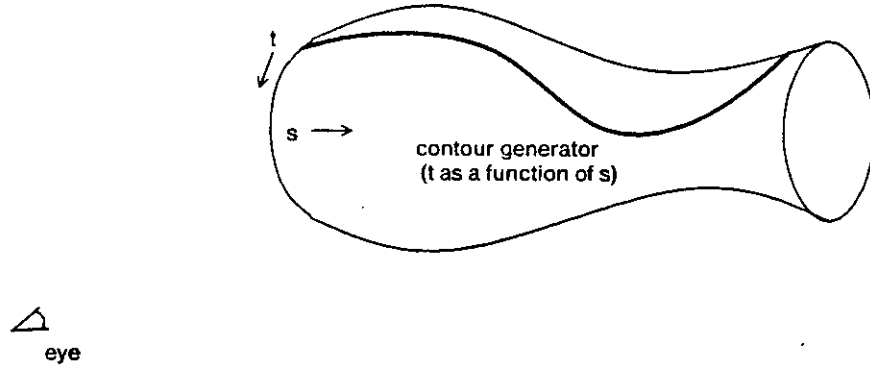
Figure 25: Contour Generator on a Right Circular SHGC

Now, since t is a function of s along the contour generator, the points $P(s,t)$ along the contour generator can be specified as $P_{CG}(s)$, a function of s only:

$$P_{CG}(s) = \left(-\cot \sigma\, r(s) \frac{dr}{ds},\ \pm r(s) \sqrt{1 - \cot^2 \sigma\, (dr/ds)^2},\ s \right)$$

and the contour generator includes points such that $v_C(t)$ is defined, i.e.

$$1 - \cot^2 \sigma \left(\frac{dr}{ds}\right)^2 \geq 0$$

$$\left| \frac{dr}{ds} \right| \leq |\tan \sigma|$$

The contour generator is not generally planar in an oblique view.

On an RCSHGC, the image of a point $P(s,t)$ is

$$I(s,t) = (r(s) \cos 2\pi t \cos \sigma + s \sin \sigma,\ r(s) \sin 2\pi t)_{xy} \tag{4-4}$$

and for a point on a contour generator,

$$I_{CG}(s) = (x_{CG}, y_{CG})(s)_{xy}$$

$$= \left(-r(s) \frac{\cos^2 \sigma}{\sin \sigma} \frac{dr}{ds} + s \sin \sigma,\ r(s) \sqrt{1 - \cot^2 \sigma\, (dr/ds)^2} \right)_{xy} \tag{4-5}$$

Further, the slope of the image contour, dy_{CG}/dx_{CG}, can be determined as a function of dr/ds using the following derivation:

$$\frac{dx_{CG}}{ds} = -\frac{cos^2 \sigma}{sin \sigma} \left(r(s) \frac{d^2 r}{ds^2} + (\frac{dr}{ds})^2 \right) + sin \sigma$$

$$= sin \sigma \left(1 - cot^2 \sigma \, r(s) \frac{d^2 r}{ds^2} - cot^2 \sigma \, (\frac{dr}{ds})^2 \right)$$

$$\frac{dy_{CG}}{ds} = \sqrt{1 - cot^2 \sigma \, (dr/ds)^2} \, \frac{dr}{ds} - (1/\sqrt{1 - cot^2 \sigma \, (dr/ds)^2}) cot^2 \sigma \, r(s) \frac{dr}{ds} \frac{d^2 r}{ds^2}$$

$$= \left(1 / \sqrt{1 - cot^2 \sigma \, (dr/ds)^2} \right) \frac{dr}{ds} \left(1 - cot^2 \sigma \, r(s) \frac{d^2 r}{ds^2} - cot^2 \sigma \, (\frac{dr}{ds})^2 \right)$$

$$\frac{dy_{CG}}{dx_{CG}} = \frac{dy_{CG}}{ds} \frac{ds}{dx_{CG}} = \left(1 / \sqrt{sin^2 \sigma - cos^2 \sigma \, (dr/ds)^2} \right) \frac{dr}{ds} \tag{4-6}$$

4.3.1 Occlusions and Singularities in Image Contours

Where $|dr/ds| > |tan \sigma|$, there will be no points on the contour generator. This causes occlusion of the contour generator from view, with resulting discontinuities in the visible contours.

To study this phenomenon, suppose we begin with the object at a side view ($\sigma = \pi/2$), and let us study the contour generator as we rotate the object towards an end view ($\sigma = 0$). At the start, $tan \sigma$ is infinite and $|dr/ds| \le tan \sigma$ for all s. There will be a single continuous contour generator on the object, which will in fact be planar (running along the top and bottom of the object) (figure 26).

As we rotate the object slightly, decreasing σ and hence $tan \sigma$, as long as $|dr/ds| \le tan \sigma$ towards that end. the contour generator will still be continuous (figure 27). However, it will no longer be planar (unless the object is also a Linear SHGC, which we will not consider further here). From equation (4-3), we see that where dr/ds is 0, $t = 1/4$, i.e. the contour generator is on "top" of the object. (Of course, there is also an identical contour generator on the bottom.) Where $dr/ds < 0$, $t > 1/4$ and the contour generator is pushed away from us; where $dr/ds > 0$, the contour generator is pulled towards us. The variation in t as we travel along the shape is expressed by:

$$\frac{dt}{ds} = \left(1 / 2\pi \cos \sigma \sqrt{sin^2 \sigma - cos^2 \sigma \, (dr/ds)^2} \right) \frac{d^2 r}{ds^2}$$

Since $|dr/ds| \le |tan \sigma|$ along the contour generators, the sign of dt/ds depends only on the sign of $d^2 r/ds^2$. Note also that $|dr/ds| > |tan \sigma|$ at the ends of the object, hence the contour generator no longer includes the ends as the object is slightly rotated away from a side view.
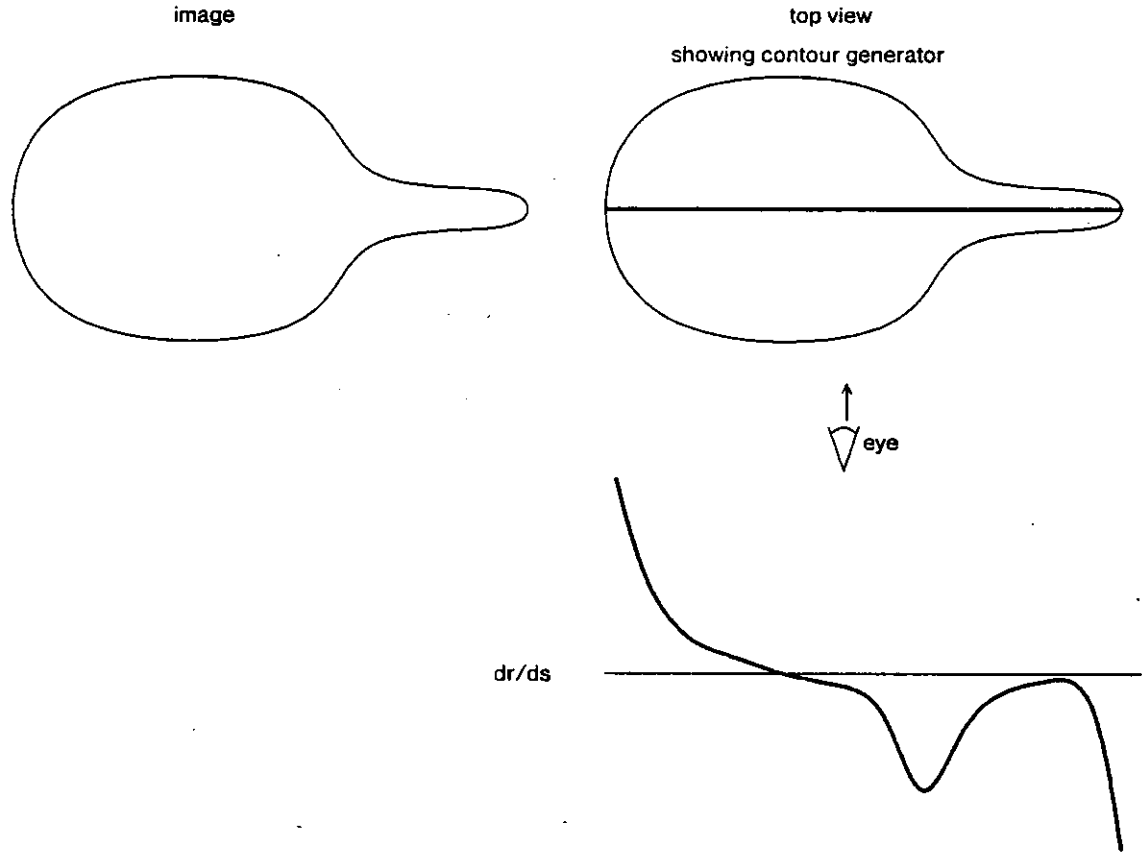
Figure 26: Contour Generator in Side View

Let us presume for the moment that the object is thinner at the near end, i.e. $dr/ds \leq 0$ everywhere. Eventually, we rotate the object so much that $dr/ds = -tan\,\sigma$ at some value of s, say s_m, where dr/ds is at a minimum (figure 28). At this value, since $dr/ds \big|_{s_m} = -tan\,\sigma$ and $d^2r/ds^2 \big|_{s_m} = 0$ (because s_m is a relative minimum for dr/ds), we have $dx_{CG}/ds \big|_{s_m} = 0$ and $dy_{CG}/ds \big|_{s_m} = 0$. Thus, the contour generator is tangent to the line of sight at s_m.

If we rotate the object yet farther, there will be an interval (s_a, s_b) around s_m in which $dr/ds < -tan\,\sigma$, i.e. for which no contour generator points exist (figure 29). What has happened is that the former, single contour generator has been split into two separate contour generators, corresponding to values of s such that $s \geq s_b$ and $s \leq s_a$. Along the contour for $s \geq s_b$, all points will be visible in the image (i.e. none are occluded by the object itself in this vicinity). Further, note that the limit of dy_{CG}/dx_{CG} is infinite as we approach s_b from above, i.e. the contour in the image becomes asymptotically vertical as we travel towards s_b: the contour thus "flares out" towards the vertical in this region.

image

top view

showing contour generator

tan $\bar{\sigma}$

dr/ds

-tan $\bar{\sigma}$

eye
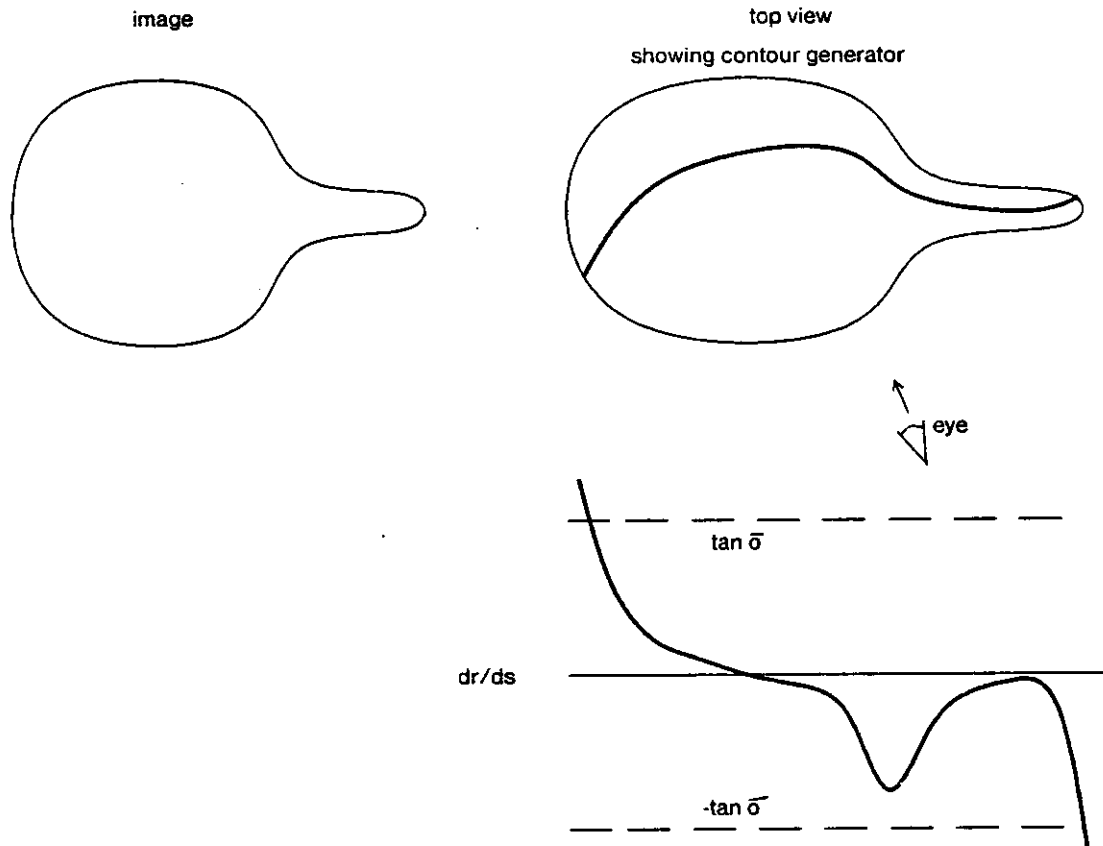
Figure 27: Contour Generator in Near-Side View

Meanwhile, along the contour for $s \leq s_a$, the object itself will occlude part of the contour generator, for values of s above some value s_c (where $s_c \leq s_a$) (segment X in figure 30). Suppose the contour generator is occluded for some s_0, where $s_c \leq s_0 \leq s_a$. Then

$$\exists s_1 \geq s_b \text{ such that } x_{CG}(s_1) = x_{CG}(s_0) \text{ and } |y_{CG}(s_1)| \geq |y_{CG}(s_0)|$$

This, unfortunately, cannot be further simplified to a condition on s without some knowledge about the behavior of $r(s)$ (the fact that $dr/ds > - \tan \sigma$ above s_b gives no useful constraint here) -- thus, segment X (in figure 30) is hard to characterize. In any event, $r(s)$ can be determined for segments A, B, and Y.

What we have seen is a single image contour splitting into two parts connected by a sort of "T" junction; the split occurred at the point at which the contour generator was tangent to the line of sight. This illustrates an important kind of "special viewpoint" for curved surfaces: If a visible arc in the scene is tangent to the line of sight, then a small variation in the viewpoint can cause a topological change in the image of the arc.

image

top view

showing contour generator

tan o̅

Sm

dr/ds

-tan o̅

eye
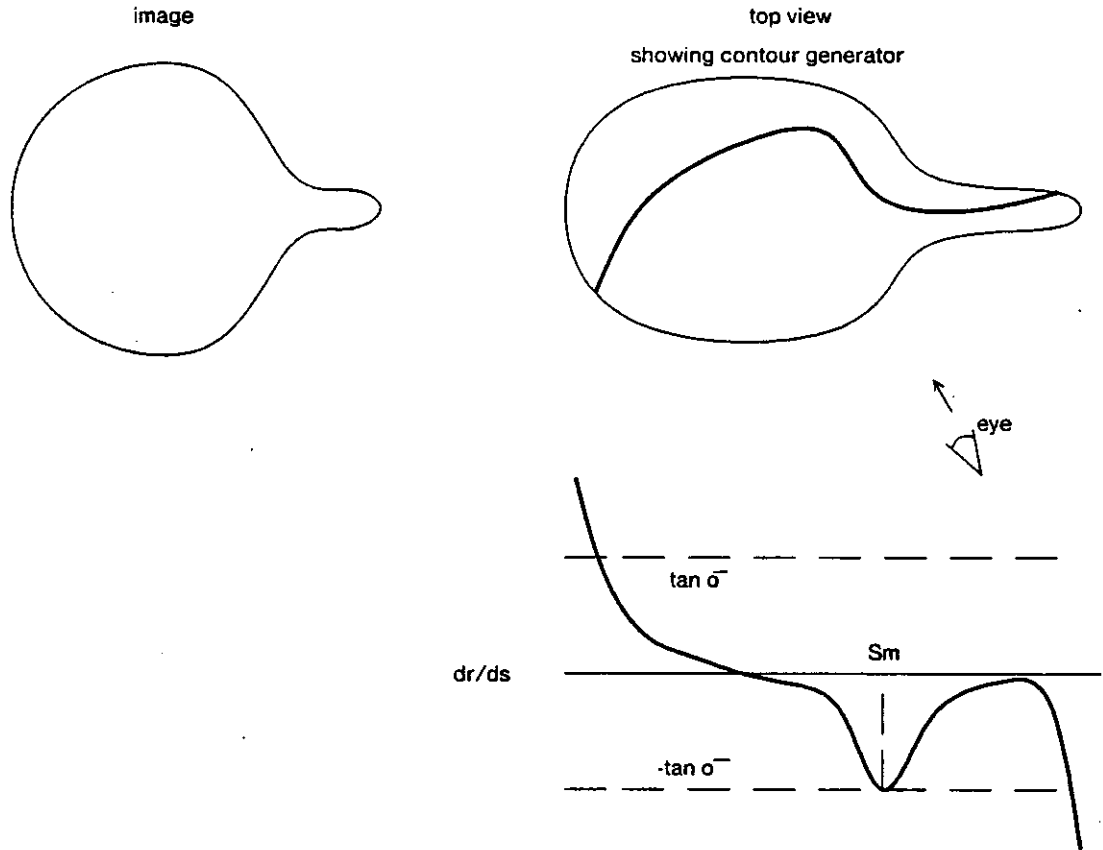
Figure 28: Contour Generator Singular When Tangent to Line of Sight

4.3.2 Cross-Sections Described by Fourier Coefficients

The use of Fourier coefficients for the functions $u_C(t)$ and $v_C(t)$ allows more complex cross-sections than circular ones to be described, while retaining some degree of mathematical tractability. Suppose, for example, that the cross-section of an RSHGC is described by one set of Fourier coefficients, which allows ellipses with arbitrary position, rotation, scale, and eccentricity. Using the notation of Kuhl and Giardina [10], we have:

$$C(t) = (u_C, v_C)(t) = (A_0 + a_1 \cos 2\pi t + b_1 \sin 2\pi t, \ C_0 + c_1 \cos 2\pi t + d_1 \sin 2\pi t)$$

so

$$\frac{du_C}{dt} = -2\pi a_1 \sin 2\pi t + 2\pi b_1 \cos 2\pi t$$

image

top view

showing contour generator

eye

tan o

Sa | Sm | Sb

dr/ds

-tan o
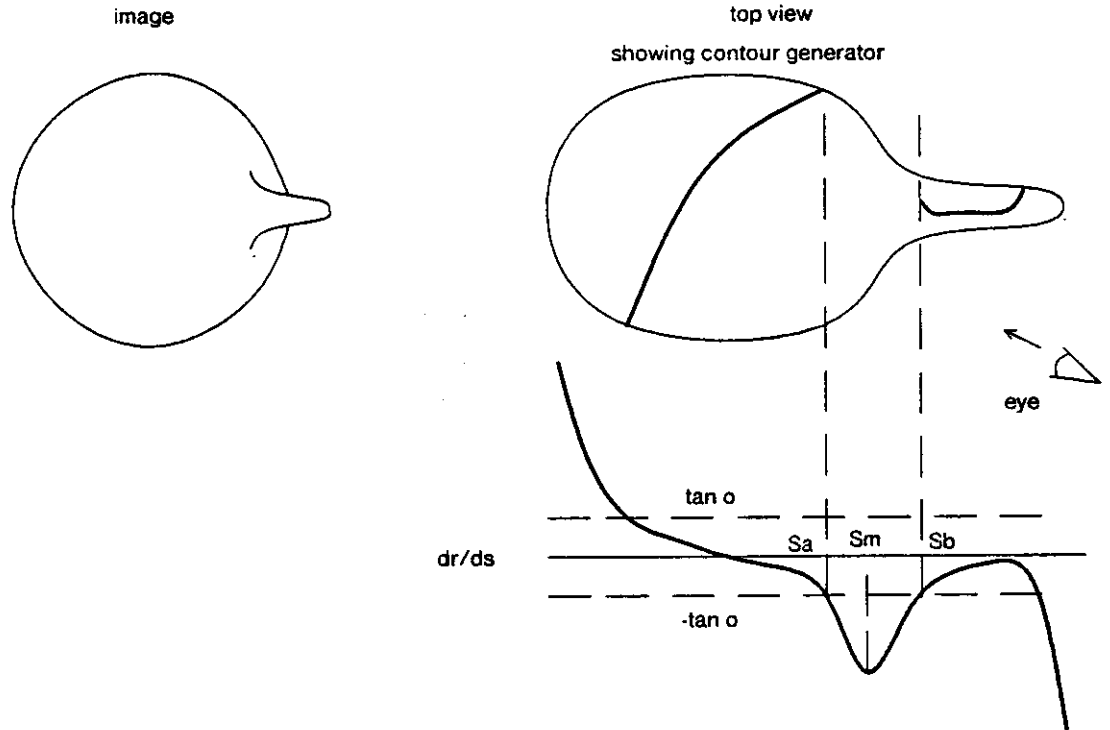
Figure 29: Contour Generator Split at Near-End View

image

r(s)

A

X

Y

B

A

Y

X

B

Sc | Sa Sm Sb
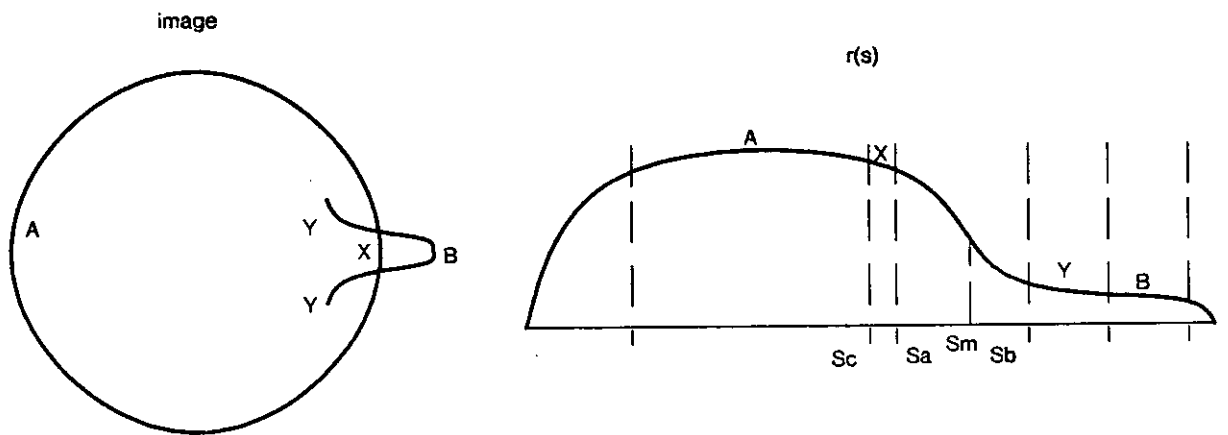
Figure 30: Contour Pieces Correspond to Disjoint Intervals of s

$$\frac{dv_C}{dt} = -2\pi c_1 \sin 2\pi t + 2\pi d_1 \cos 2\pi t$$

$$h(t) = 2\pi \left((A_0 d_1 + C_0 b_1) \cos 2\pi t - (A_0 c_1 + C_0 a_1) \sin 2\pi t + a_1 d_1 + b_1 c_1 \right)$$

The points on the contour generators must obey:

$$0 = \sin \sigma \, (d_1 \cos 2\pi t - c_1 \sin 2\pi t)$$

$$- \cos \sigma \frac{dr}{ds} \left((A_0 d_1 + C_0 b_1) \cos 2\pi t - (A_0 c_1 + C_0 a_1) \sin 2\pi t + a_1 d_1 + b_1 c_1 \right)$$

$$t = (1 / 2\pi) \sin^{-1} \left((-eg + f\sqrt{e^2 + f^2 - g^2}) / (e^2 + f^2) \right)$$

where

$$e = -c_1 \sin \sigma + (A_0 c_1 + C_0 a_1) \cos \sigma \frac{dr}{ds}$$

$$f = d_1 \sin \sigma - (A_0 d_1 + C_0 b_1) \cos \sigma \frac{dr}{ds}$$

$$g = -(a_1 d_1 + b_1 c_1) \cos \sigma \frac{dr}{ds}$$

Since t has been expressed here as a function of s along the contour generators, we can presumably express points along the contour generators as $P_{CG}(s)$ and contour points as $I_{CG}(s)$. Much of the following analysis of Right Circular SHGCs will therefore be applicable for RSHGCs with arbitrary ellipses as cross-sections; while the closed-form expressions will be complex, actual numeric analysis should not be difficult.

For cross-sections described by two sets of Fourier coefficients (i.e. A_0, a_1, a_2, b_1, b_2, C_0, c_1, c_2, d_1, d_2), analysis is yet more difficult but still conceivable. For additional coefficients, however, such closed-form analysis seems beyond tractability.

4.4 Contour and Silhouette Analysis for Right Circular SHGCs

In image understanding, we are faced with the problem of analyzing image contours rather than predicting them. We can accomplish this task using the above description of the properties of contour generators.

Suppose we have a line drawing consisting of visible (i.e. unoccluded) contours, each of which is the image of some contour generator on a Right Circular SHGC. By analyzing the contours, we can construct a description of the solid shape portrayed.
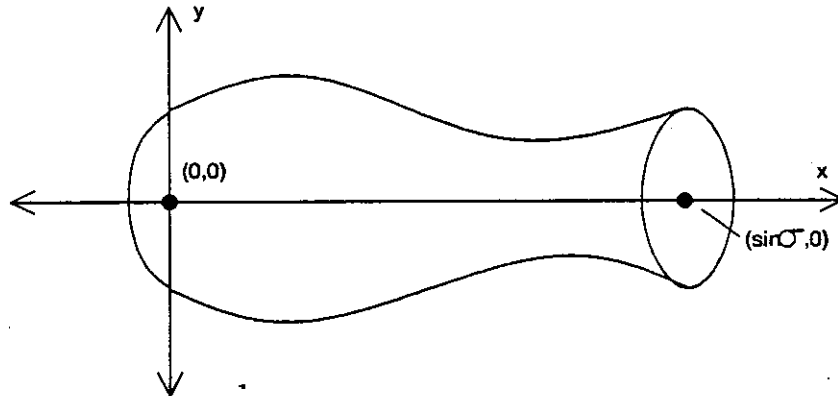
Figure 31: Aligned Image of an SHGC

First, we need to determine the viewing angle σ and to align the image as in figure 31, so the images of the endpoints of the axis $A(0)$ and $A(1)$ are at $(0,0)_{xy}$ and $(sin\ \sigma,\ 0)_{xy}$, respectively; this conforms to the imaging model presented previously. Then, we can analyze the contours to recover the shape; for a Right Circular SHGC, we need only determine $r(s)$, the radius function, to have a complete description of the shape.

We will begin by addressing the latter problem -- analysis of contours when the image is aligned and σ known. Then, we will examine how to determine σ and perform the alignment.

4.4.1 Contour Analysis

Along a contour generator of a Right Circular SHGC, recall that equations (4-5) and (4-6) give $x_{CG}(s)$, $y_{CG}(s)$, and dy_{CG}/dx_{CG} as functions of s, $r(s)$, and dr/ds. These allow us to solve for s, $r(s)$, and dr/ds, the shape description, as functions of $x_{CG}(s)$, $y_{CG}(s)$, and dy_{CG}/dx_{CG}, which can be measured in the image. We obtain:

$$s = \frac{x_{CG}(s) - y_{CG}(s)\ cos^2\ \sigma\ (dy_{CG}/dx_{CG})}{sin\ \sigma}$$

$$r(s) = y_{CG}(s)\ \sqrt{1 + cos^2\ \sigma\ (dy_{CG}/dx_{CG})^2}$$

$$\frac{dr}{ds} = \left(sin\ \sigma\ /\ \sqrt{1 + cos^2\ \sigma\ (dy_{CG}/dx_{CG})^2}\ \right) \frac{dy_{CG}}{dx_{CG}}$$

image x,y   description r(s)
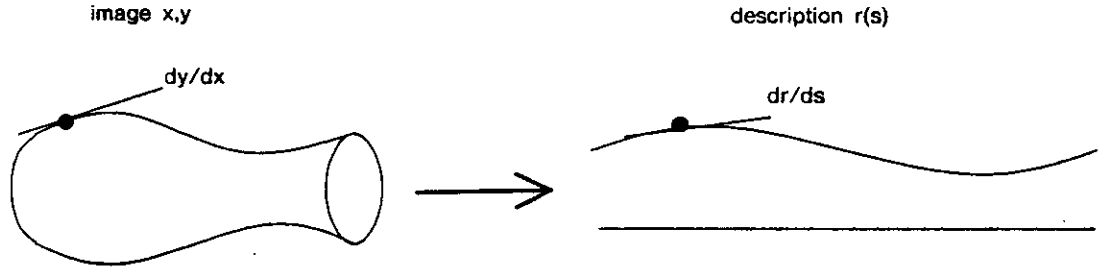
Figure 32: Contour Analysis Results in Shape Description

So, given any contour point $(x_{CG}(s), y_{CG}(s))_{xy}$, and the slope dy_{CG}/dx_{CG} of the contour at that point, we can determine s, $r(s)$, and dr/ds at that point. By doing this for all contour points, we can determine as much as possible about $r(s)$ from the image (figure 32).

As stated earlier, this analysis presumes that σ is known and that the image is appropriately aligned.

4.4.2 Occluded Contours and Silhouettes

We have seen how to analyze contours to determine values of $r(s)$; now, we will discuss how much of $r(s)$ can be reconstructed in this manner (i.e. over what range of values of s). As we already know, there is a contour generator only where $|dr/ds| \leq |tan\ \sigma|$; values of s for which $|dr/ds| > |tan\ \sigma|$ therefore do not correspond to any points on a contour generator, and $r(s)$ cannot be determined for these values by examination of image contours. In addition, as described in section 4.3.1, the object itself may occlude portions of the contour generator from view.

For analyzing a silhouette, exactly the same methods and conditions apply, except that, using the notation of section 4.3.1, the contour for $s \leq s_c$ will render invisible the contour for $s \geq s_b$ which lies to the left of $I_{CG}(s_c)$; thus, in figure 30, only segments A and B will be visible. This may be stated as follows: The contour generator for s_0 is occluded or invisible if

$$\exists s_1 \neq s_0 \text{ such that } x_{CG}(s_1) = x_{CG}(s_0) \text{ and } |y_{CG}(s_1)| \geq |y_{CG}(s_0)|$$

The only difference between this case and the above discussion for $s \leq s_a$ is that the requirement $s_1 \geq s_b$ has been generalized to $s_1 \neq s_0$. Thus, silhouettes are simply images of contours in which certain portions of some contours are not visible.

If $dr/ds > 0$, the situation is just the above viewed from the opposite direction (i.e. segments A, B,

and X in figure 30 will be visible, and segment Y will be occluded). In this case, when the contour generator splits, the arc for $s \leq s_a$ is still occluded, but the arc for $s \geq s_b$ is a closed curve in the image rather than flaring out as above. Silhouette analysis will be identical; indeed, the silhouette of an object is identical (to within a reflection) viewed from opposite directions.

In any of these cases, there will be an interval of s over which $r(s)$ cannot be computed, say (s_i, s_j). However, we can compute $r(s_i)$, $r(s_j)$, $dr/ds \big|_{s_i}$, and $dr/ds \big|_{s_j}$. For practical image analysis, it is possible to estimate $r(s)$ over (s_i, s_j) by fitting a function which conforms to these constraints. For example, a cubic polynomial can be fit to the data:

$$r(s) = as^3 + bs^2 + cs + d$$

so

$$\frac{dr}{ds} = 3as^2 + 2bs + c \quad .$$

Then the following system of linear equations can easily be solved to determine the values of a, b, c, and d:

$$
\begin{bmatrix} r(s_i) \\ r(s_j) \\ dr/ds \big|_{s_i} \\ dr/ds \big|_{s_j} \end{bmatrix}
=
\begin{bmatrix} s_i^3 & s_i^2 & s_i & 1 \\ s_j^3 & s_j^2 & s_j & 1 \\ 3s_i^2 & 2s_i & 1 & 0 \\ 3s_j^2 & 2s_j & 1 & 0 \end{bmatrix}
\begin{bmatrix} a \\ b \\ c \\ d \end{bmatrix}
$$

4.4.3 Aligning the Image

The above analysis has presumed that we know the viewing angle σ and have aligned the images of the axis endpoints $A(0)$ and $A(1)$ onto $(0,0)_{xy}$ and $(sin\ \sigma, 0)_{xy}$, respectively. We will now address the problems of aligning the image and determining σ.

Suppose we are given an image of the contours of a Right Circular SHGC, arbitrarily scaled, rotated, and translated, and viewed from an unknown angle. We can immediately determine the image of the axis, since this will be an axis of symmetry in the image, and rotate the image so this is horizontal. By translating the image, this axis can be made to line up with the x-axis. Brooks [3] and Marr and Nishihara [12] discuss this issue of finding the image of the axis of a generalized cylinder.

We must next determine which end of the object is nearer, so this can be placed on the right as in our imaging model. If the left end is closer, we will need to reflect the image about the y-axis, or equivalently rotate it 180° about the origin.

We must also determine σ and find the images of the axis endpoints. Determining σ is more important, since it affects both the image alignment and the shape of the reconstructed function $r(s)$. The axis endpoints, on the other hand, affect only the scale and shifting (along s) of $r(s)$.
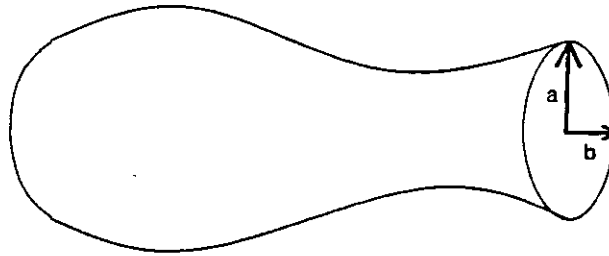
Figure 33: RCSHGC With Near End Flat

If the closer end of the object is flat as in figure 33, i.e. $r(1) > 0$, then the edge of the cross-section at that end will produce a contour in the image, which will be a vertically elongated ellipse. This is a very useful configuration, since we can easily determine which end of the object is closer. Then, we know that the center of the ellipse must be the image of the axis endpoint $A(1)$; further, we can compute the viewing angle σ from the eccentricity of the ellipse, using $cos\ \sigma\ =\ b/a$, where a and b are the semimajor and semiminor axis lengths, respectively.

If the farther end of the object is flat and not occluded, i.e. $r(0) > 0$ and $dr/ds\ \big|_0 < tan\ \sigma$, then we will se exactly half of an ellipse, which can be analyzed as above to determine which end of the object is farther, the image of $A(0)$, and σ.

If neither end can be analyzed as above, we may be able to determine whether any "T"-shaped occlusions occur along the contour; if so, the occluding contour generator is on the nearer portion of the object. Failing this, we cannot from contours alone decide which end of the object is nearer. Fortunately, there are many other potential sources for alignment information, such as the object's length or width, or surface normals as determined by photometry or range data.

It should be noted that, for a curved surface, scaling the figure along s and altering the viewing angle σ are *not* complementary; i.e. we cannot keep the image contours constant by altering the viewing angle and compensating with elongation of the object. The reason is that elongation does not alter the position of the contour generators on the shape, but when the viewing angle is altered, the contour generators "creep" along the surface to a different position. This occurs because within

a local neighborhood of a point, the angle between the surface normal N and the viewing direction F varies. This may be contrasted, for example, with polyhedra under orthography, in which this angle is constant, causing contour generators to remain in place, and allowing elongation and rotation of the viewing direction to compensate to keep the image constant. The dependance of contour generator position upon the viewing angle is the reason that s and $r(s)$ depend upon σ in a complicated manner rather than being, say, proportional to $\sin \sigma$ or $\cos \sigma$.

4.5 Contour and Silhouette Analysis for Other RSHGCs

There are several steps to be performed when analyzing contours of any Right SHGC, as illustrated in the above discussion of Right Circular SHGCs:

1. Finding the image of the axis line.

2. Finding the images of the axis endpoints.

3. Deciding which end of the axis is nearer.

4. Determining the viewing angle, σ.

5. Determining the cross-section, $C(t)$.

6. Determining the radius function, $r(s)$.

Steps 1-4 are required to align the image; then, contour analysis can proceed to perform steps 5-6.

If the near end of the RSHGC is flat and bounded by a sharp edge, i.e. $r(1) > 0$ and $\frac{dr}{ds}\big|_1$ is finite, its edge produces a contour which can be analyzed to assist in steps 1, 2, and 4, and to solve 3 and 5. If the near end is not flat but the far end is flat and produces a visible contour, it can be used to assist in steps 1, 2, 4, and 5, and to solve 3.

For solving step 1, we can also use the fact that, for any two points with the same s-value but different t-values, the tangents to the surface in the direction of increasing s will intersect at a point on the axis (figure 34). This can be seen by noting that on an RSHGC, for given values of s and t,

$$P(s,t) = (u_C(t)\, r(s),\, v_C(t)\, r(s),\, s)$$

$$\frac{\partial P}{\partial s} = (u_C(t)\, \frac{dr}{ds},\, v_C(t)\, \frac{dr}{ds},\, 1)$$

So the vector from P in the direction $\partial P/\partial s$ intersects the axis at the point
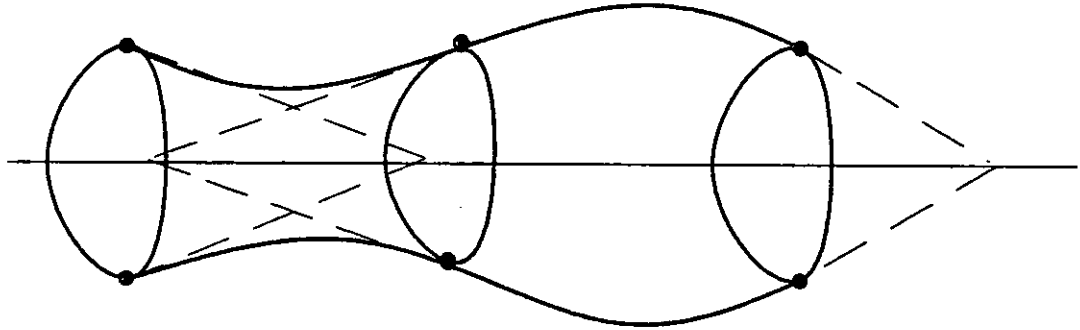
Figure 34: Tangents at Corresponding Points Intersect on the Axis

$$\left(0, \ 0, \ s \ - \ \frac{r(s)}{dr/ds} \right)$$

Since this is independent of t, we can take two points with the same s-coordinate, draw the respective tangents $\partial P/\partial s$, and the intersection of these latter will be some point on the axis. In the image, the same relationship holds, using tangents to visible contours, providing the contour generators are arcs of constant t (so that their tangents are in fact $\partial P/\partial s$). Of ocurse, to make use of this phenomenon, some means would be required for finding points with the same s-coordinate. Surface markings or knowledge of $C(t)$ might make this possible.

4.5.1 Contours of Right Linear SHGCs

Right Linear SHGCs have some additional properties that can aid in contour analysis. First, recall that equation (4-2) gives the condition satisfied by points on the contour generator of a Right Linear SHGC. This is a condition only on t, so the contour generators are curves of constant t. This is implied also by the Corresponding Normal Theorem, $\partial N/\partial s = (0,0,0)$ for an LSHGC.

So, each contour generator is a straight line of constant t on the surface. These lines must all pass through the apex of the shape, so any two such contours in the image must intersect at the image of the apex. This is one point on the axis; by the the Pivot Theorem, the axis can then be defined in any direction passing through this point. On the other hand, it may be very difficult to determine σ unless the cross-section function $C(t)$ is known in advance, since so little information is contained in the image contours.

Interestingly, the contour generators in an oblique view need not correspond to relative maxima

side view   oblique view   end view
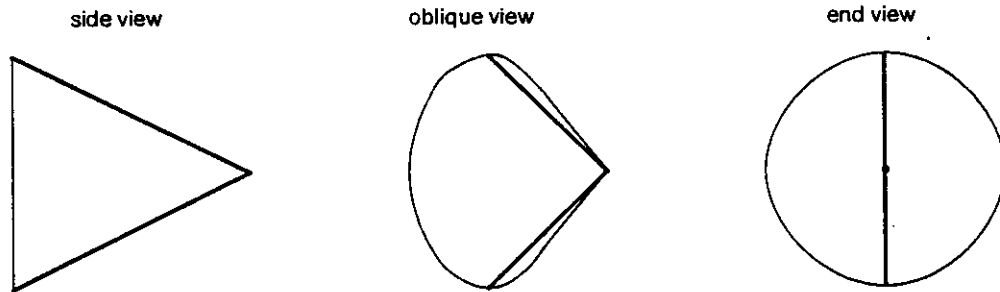
Figure 35: Contour Generators Need Not Be At Vertical Extrema

and minima of $v_c(t)$, i.e. the contour generators need not be on the "top" and "bottom" of the shape, but may occur where $dv_c/dt \neq 0$. For example, figure 35 shows a cone with a vertical stripe. In an oblique or end view, parts of the surface will be visible on both sides of the stripe.

On a Right Linear SHGC, there will be no partially occluded contours (except possibly at the near end of the shape), since all contour generators are linear.

4.5.2 Contours of Right Polygonal SHGCs

A Right Polygonal SHGC has two types of contour generators: faces tangent to the line of sight, and creases. A contour generator on a face obeys $0 = N \cdot F$, so

$$\frac{dr}{ds} = \frac{m_v \tan \sigma}{m_u b_v - m_v b_u}$$
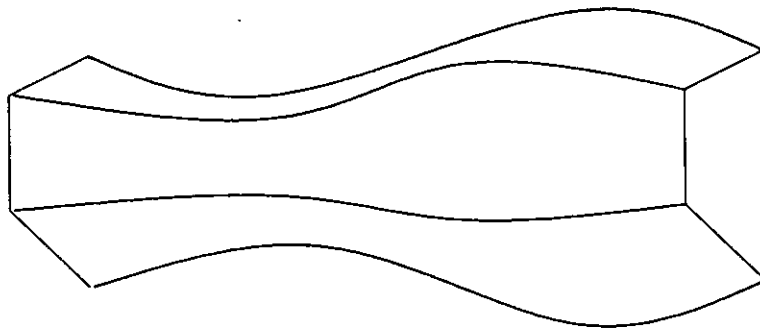
Figure 36: Crease Contours for a Right Polygonal SHGC

In addition, each vertex of the polygonal cross-section creates a crease on the surface which might be visible in the image, so each crease is in effect a contour generator (though not normally tangent to the line of sight) (figure 36). If $C(t_0) = (u_0, v_0)$ is a vertex, then

$$P(s,t_0) = P_{CG}(s) = (u_0 r(s), v_0 r(s), s)$$

$$I(s,t_0) = I_{CG}(s) = (x_{CG}, y_{CG})(s)_{xy} = (u_0 r(s) \cos \sigma + s \sin \sigma, v_0 r(s))_{xy}$$

Since crease contours provide so much information in the image of a Right Polygonal SHGC, we will limit our attention to creases in the following discussion.

First, we note that tangents to crease contours for corresponding points intersect at a point on the image of the axis, just as described above for contour generators on an RSHGC. It is especially easy to find pairs of corresponding points on a Polygonal RSHGC, as in figure 37. Suppose $C(t_1) = (u_1, v_1)$ and $C(t_2) = (u_2, v_2)$ are vertices corresponding to visible crease contours. Then for any s, the slope of the image line joining $I(s,t_1)$ and $I(s,t_2)$ is:

$$\frac{\Delta y}{\Delta x} = \frac{v_2 r(s) - v_1 r(s)}{u_2 r(s) \cos \sigma + s \sin \sigma - u_1 r(s) \cos \sigma - s \sin \sigma} = \frac{v_2 - v_1}{(u_2 - u_1) \cos \sigma}$$
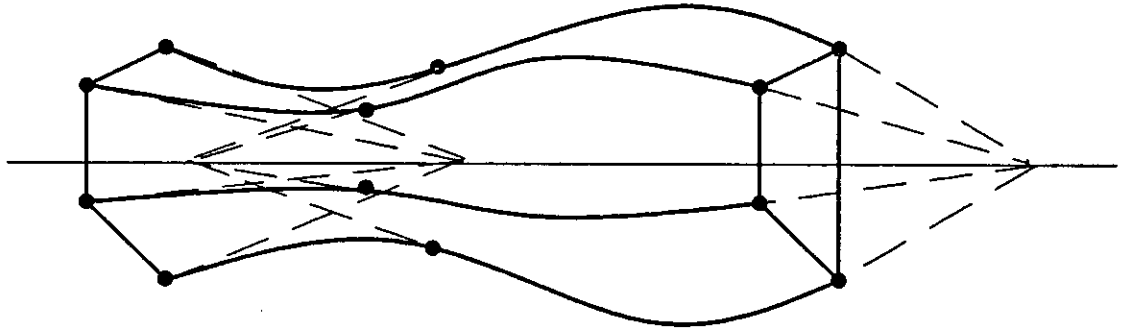
Figure 37: Tangents of Crease Contours Intersect on the Axis

which is independent of s. Thus, the slope of the line joining corresponding points on the two crease contours is constant. By examining either end of the PRSHGC, we can pick two vertices, find the slope of the line joining these, and thus find pairs of corresponding points all along the associated crease contours. In this way, the image of the axis can be found. This will only fail in the event that the crease contours have constant slope, i.e. the shape is also a Linear SHGC. In such a case, however, as described above, the apex is easily found, and other points on the axis can be arbitrary.

Unfortunately, there seems to be little direct evidence in the crease contours to indicate the viewing angle σ. Similarly, while the authors believe the images of the axis endpoints ought to be easily determined, no direct method has yet been found. Perhaps this problem is deceptive in its apparent simplicity. In any event, at the present time, outside knowledge seems necessary in order to align the image for contour analysis.

Supposing that the image has in fact been aligned in accordance with our imaging model, the analysis of the crease contours is straightforward, and is based on these formulae:

$$\frac{dx_{CG}}{ds} = u_0 \cos \sigma \frac{dr}{ds} + \sin \sigma$$

$$\frac{dy_{CG}}{ds} = v_0 \frac{dr}{ds}$$

$$\frac{dy_{CG}}{dx_{CG}} = \frac{v_0 \, (dr/ds)}{\sin \sigma + u_0 \cos \sigma \, (dr/ds)}$$

So, at any point $I_{CG}(s) = (x_{CG}, y_{CG}) \, (s)$,

$$s = \frac{v_0 \, x_{CG}(s) - u_0 \, y_{CG}(s) \cos \sigma}{v_0 \sin \sigma}$$

$$r(s) = \frac{y_{CG}(s)}{v_0}$$

$$\frac{dr}{ds} = \frac{\sin \sigma \, (dy_{CG}/dx_{CG})}{v_0 - u_0 \cos \sigma \, (dy_{CG}/dx_{CG})}$$

A "special viewpoint" will not normally arise with crease contours, since a crease contour is tangent to the line of sight only if $dx_{CG}/ds = 0$ and $dy_{CG}/ds = 0$, i.e. in one of two situations:

- $dr/ds = 0$ and $\sigma = 0$: an end view

- $v_0 = 0$ and $dr/ds = -\tan \sigma \, / \, u_0$: a vertex on the u-axis, which creates a horizontal crease whose image cannot occlude (nor be occluded by) that of any other crease.

4.6 Contour Generators in Two Views

eye 1

eye 2

contour generator 2   contour generator 1
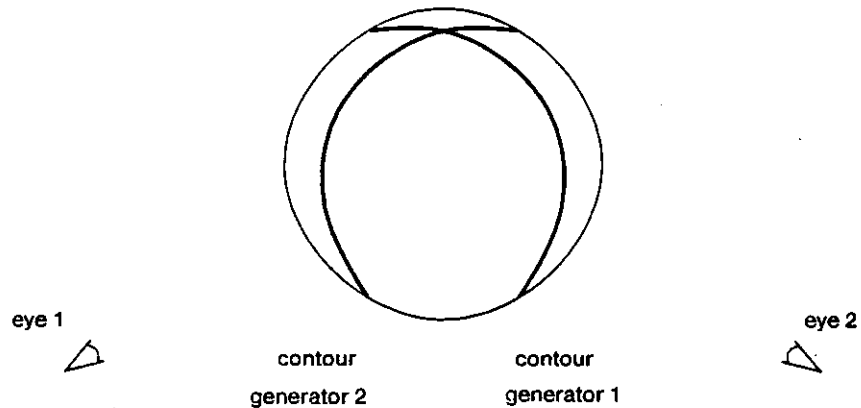
Figure 38: Contour Generators From Two Points of View

image   scene

eye
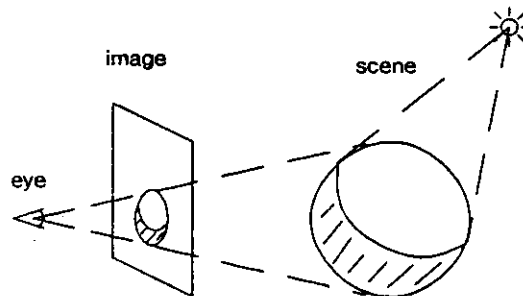
Figure 39: Shadow Line is a Contour Generator for the Light Source

Suppose we have an object which is being viewed by two cameras, from two different directions. What will the contour generators from one point of view look like in the image as seen from the other point of view? This is an important question for image understanding, since it bears on three different imaging situations:

- *Stereo* -- Commonly, two different cameras are viewing the same scene, and corresponding points in the two views must be found. However, the contour generators from one view generally do not match the contour generators from the other view (figure 38). So, we need to determine how the contour generators from one image appear in the other image.

- *Range Finders* -- A common type of range-finder has a separate illuminator and camera,

and uses triangulation to determine the distance to various points in the scene. However, points occluded from illumination are generally not the same as the points occluded from the camera. Since the boundaries of occluded areas are the projections of contour generators onto background objects, we want to know how the contour generators as pertains to the illuminator are viewed by the camera.

● *Shadow Geometry* -- In images with strong light sources and low ambient ("diffuse") light levels, shadows will frequently appear. If an object is illuminated, there will appear a (usually highly visible) "shadow line" (also called "terminator") separating the illuminated part of the object from the self-shaded part of the object (the part facing away from the light source) (figure 39). This shadow line is simply a contour generator from the point of view of the light source, and we want to know how to analyze its image as seen by the camera.
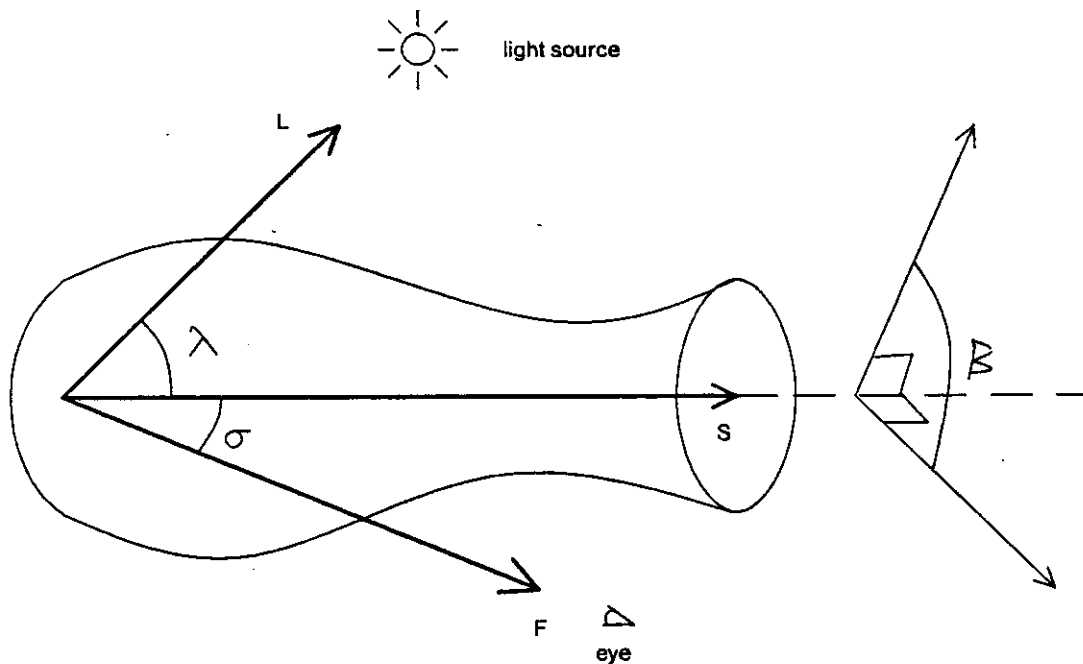
Figure 40: Two Angles Define the Illumination Direction

Since this last situation is highly intuitive, we will couch the following discussion in terms of shadows. We will use $L = (l_w, l_v, l_s)$ to denote the direction pointing at the light source. The angle of illumination, λ, will represent the angle from L to S, and β will be the dihedral angle at S from the S-F plane to the S-L plane (figure 40). Then

$$L = (l_w, l_v, l_s) = (-\cos \beta \sin \lambda, \sin \beta \sin \lambda, \cos \lambda)$$

On a Right SHGC, the shadow lines must obey $N \perp L$, i.e.

$$0 = N \cdot L$$

$$= \cos \beta \sin \lambda \frac{dv_C}{dt} + \sin \beta \sin \lambda \frac{du_C}{dt} + h(t) \cos \lambda \frac{dr}{ds}$$
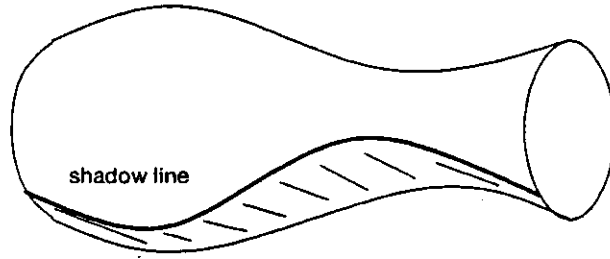
Figure 41: Shadow Line on a Right Circular SHGC

In the case of a Right Circular SHGC, as shown in figure 41, the shadow line condition simplifies to:

$$0 = \sin \lambda \cos (2\pi t - \beta) + \cos \lambda \frac{dr}{ds}$$

$$t = \frac{\beta}{2\pi} + \frac{1}{2\pi} \cos^{-1} \left(-\cot \lambda \frac{dr}{ds} \right)$$

This is similar to the relation between s and t for contour generators seen from F, except for the addition of the term $\beta/2\pi$ which represents the shift in t-coordinates due to the dihedral illumination angle relative to the axis. On the shadow line,

$$u_C(t) = \cos 2\pi t = -\cos \beta \cot \lambda \frac{dr}{ds} - \sin \beta \sqrt{1 - \cot^2 \lambda \, (dr/ds)^2}$$

$$v_C(t) = \sin 2\pi t = \sqrt{1 - u_C(t)^2}$$

$$= \sqrt{\cos^2 \beta - \cos 2\beta \cot^2 \lambda \, (dr/ds)^2 - \sin 2\beta \cot^2 \lambda \, (dr/ds)^2 \, [1 - \cot^2 \lambda \, (dr/ds)^2]^{1/2}}$$

From this point, while derivation of $P(s)$, $I(s)$, and dx/ds is achievable, the derivation of dy/ds, and hence dy/dx, s, $r(s)$, and dr/ds seems to be very difficult. The exhaustive analysis of such image contours is thus beyond our reach at present, even for the relatively simple case of Right Circular SHGCs.

One conclusion, however, can be reached: since the interval of uncertainty of $r(s)$ decreases with an increase in the viewing angle σ or the illumination angle λ, we get additional information from the shadow line for Right Circular SHGC only when $\lambda > \sigma$, i.e. the illumination direction is more nearly perpendicular to the axis than is the line of sight.

Under perspective projection from the second (illuminator) point of view, for example if the light source is a point source rather than being infinitely far away, the illumination direction becomes $L(s,t)$, a function of s and t, and shadow-line analysis is far more difficult.

4.7 Analysis of Surface Normals

In an image understanding situation, information about surface normals may be available from such sources as photometric analysis, texture analysis, shadow geometry, or range-finder data. Surface normals can be used to aid in the analysis of an image of an SHGC.

4.7.1 Individual Surface Normals of an RCSHGC
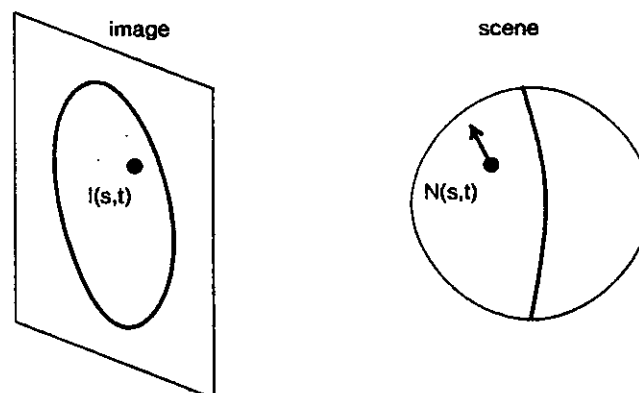
Figure 42: Knowledge of a Single Surface Normal

We will begin with the simplest case: a single surface normal of a Right Circular SHGC (figure 42). With the image aligned as above, let $I(s,t)$ be the image point at which the surface normal is given. Equation (4-4) above gives $I(s,t)$ as a function of s, t, $r(s)$, and σ.

The surface normal itself has two degrees of freedom, specifying its direction, since its length is irrelevant. The surface normal of an RCSHGC is:

$$N(s,t) = (\cos 2\pi t)\ W + (\sin 2\pi t)\ V - (dr/ds)\ S$$

$$= \left(\cos \sigma \cos 2\pi t - \sin \sigma \frac{dr}{ds},\ \sin 2\pi t,\ -\sin \sigma \cos 2\pi t - \cos \sigma \frac{dr}{ds}\right)_{xyz}$$

We can describe the direction of the normal by its *gradient* [15]: if the normal vector is $N(s,t) = (n_x, n_y, n_z)\ (s,t)_{xyz}$, then its gradient is

$$G(s,t) = (p,q)\ (s,t)$$

$$p(s,t) = \frac{n_x}{n_z} = \frac{\sin \sigma\ (dr/ds) - \cos \sigma \cos 2\pi t}{\sin \sigma \cos 2\pi t + \cos \sigma\ (dr/ds)} \qquad (4\text{-}7)$$

$$q(s,t) = \frac{n_y}{n_z} = \frac{-\sin 2\pi t}{\sin \sigma \cos 2\pi t + \cos \sigma\ (dr/ds)} \qquad (4\text{-}8)$$

When $I(s,t)$ and $G(s,t)$ are known, therefore, we have four equations (x, y, p, q) in five unknowns $(s, t, r(s), dr/ds, \sigma)$. Thus, if one of the unknowns is given, the other four can be determined.

Suppose, for example, that the viewing angle σ has been determined by some other means. Then we can solve for the four remaining unknowns: first p and q are used to determine t and dr/ds; then y is used to determine $r(s)$; finally, x is used to solve for s. The resulting equations are:

$$s = \frac{xq - y \cos \sigma\ (p \cos \sigma - \sin \sigma)}{q \sin \sigma}$$

$$t = \frac{1}{2\pi} \sin^{-1} \frac{q}{\sqrt{k}}$$

$$r(s) = \frac{y \sqrt{k}}{q}$$

$$\frac{dr}{ds} = \frac{-1 - \sin \sigma\ (p \cos \sigma - \sin \sigma)}{\cos \sigma\ k^{1/2}}$$

where

$$k = (p \cos \sigma - \sin \sigma)^2 + q^2$$

Thus, from a single surface normal on a Right Circular SHGC, when the viewing angle is known, we can determine the position of the corresponding point on the surface (s and t), the radius at that point ($r(s)$), and the derivative of the radius function at that point (dr/ds) (figure 43).
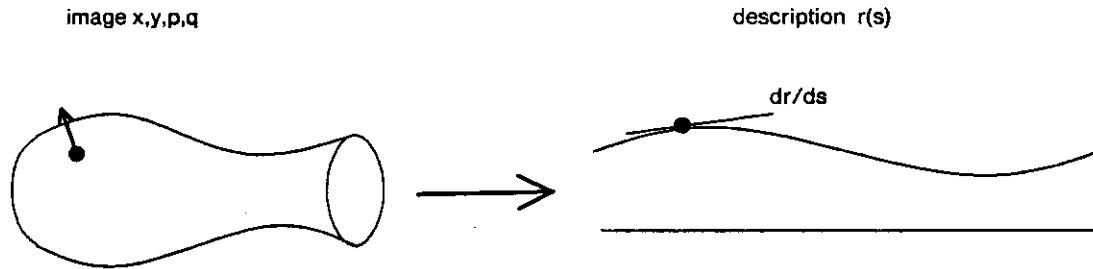
Figure 43: Analyzing a Single Surface Normal

4.7.2 Aligning the Image for Analysis of Surface Normals

The above analysis holds only when the image is aligned in accordance with these rules:

1. The image of the axis is on the horizontal x-axis in the image.
2. The viewing angle σ is known.
3. The image of the far axis endpoint is at $(0,0)_{xy}$, and the near endpoint image is at $(sin \sigma, 0)_{xy}$.

In general, condition (1) will not be difficult to establish, but conditions (2) and (3) may require considerable analysis. We will call an image *partially aligned* if it conforms to (1), and *aligned* or *completely aligned* if it conforms to (1)-(3). In addition, for partial alignment, we will require that the images of the axis endpoints are at $(0,0)_{xpyp}$ and $(1,0)_{xpyp}$ (figure 44). If the coordinates of a partially aligned image are denoted x_p and y_p, then they are related to aligned coordinates x and y by the formula:

$$(x_p, y_p)_{xpyp} = \left(\frac{x}{sin\ \sigma}, \frac{y}{sin\ \sigma}\right)$$

The division of both coordinates is required to preserve the relative proportions of the shape and its description.

To completely align an image which is already partially aligned, it is necessary to determine the endpoints of the axis and the viewing angle. The axis endpoints may be completely invisible, thus presenting an unavoidable ambiguity; also, in the event that the axis endpoints cannot in fact be determined, the only penalty is a translation and scaling of $r(s)$ relative to s, which is probably only a minor problem for shape recognition. However, the determination of the viewing angle is an interesting problem in its own right, and the penalty for guessing wrong may be a considerable distortion of $r(s)$. Therefore, we will concentrate on the problem of determining the viewing angle.
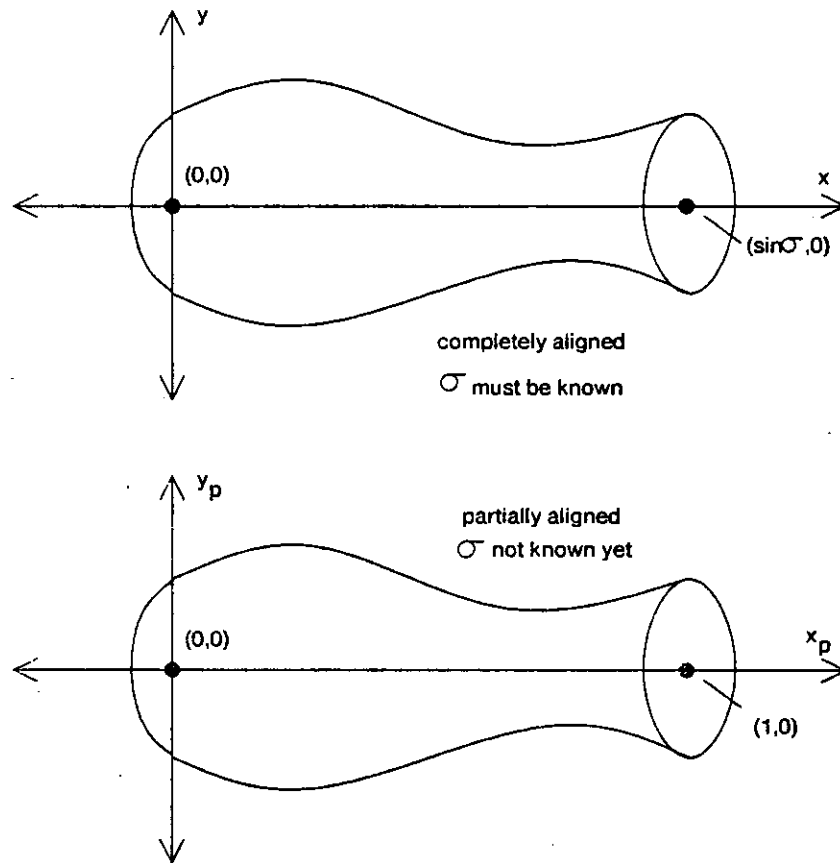
Figure 44: Complete and Partial Alignment of the Image
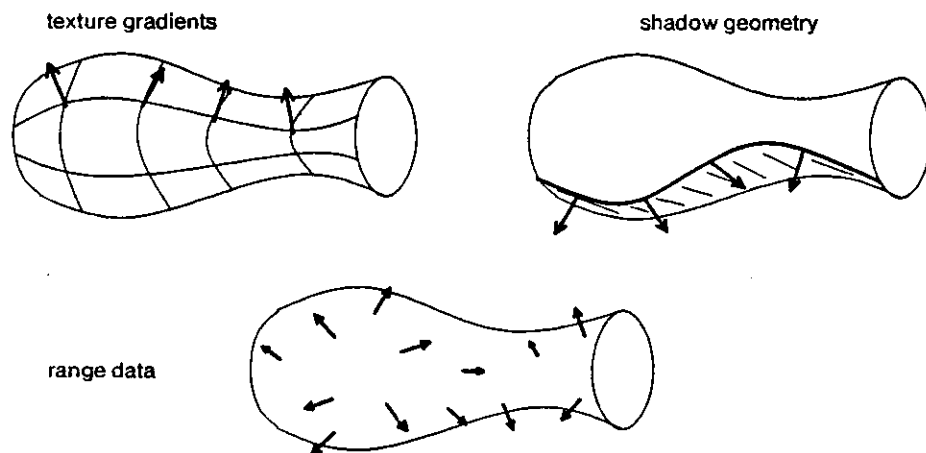
Figure 45: Sources of Knowledge About Surface Normals

In real images, where surface normals of curved surfaces are being analyzed, one or more of the following types of information are frequently being used (figure 45):

- texture gradients -- Using texture gradients, including photometric analysis, a one-dimensional constraint can be determined between the components p and q of the surface gradient [7, 8, 9].

- shadow geometry -- Using shadow geometry, the surface normal can be determined at every point along the shadow line [17].

- range data -- Using a range-finder, the raw distance data can be used to determine approximate surface normals at many points (almost every point) in the image.

While analysis of the constraints produced by texture gradients is beyond the scope of this paper, the following sections explore the latter two kinds of information and how they can be used to determine the viewing angle σ.

The discussion herein will be limited to Right Circular SHGCs, for the sake of simplicity.

4.7.3 Cross-Sections For a Given Surface Normal

Suppose we have a partially aligned image of a Right Circular SHGC, and suppose further that we are given a single surface normal. We know its position in the image, given by:

$$x(s,t) = r(s) \cot \sigma \cos 2\pi t + s$$

$$y(s,t) = \frac{r(s) \sin 2\pi t}{\sin \sigma}$$

and the gradient of the surface normal, p and q as previously defined. (Note that p and q are the same for aligned and partially aligned images.)
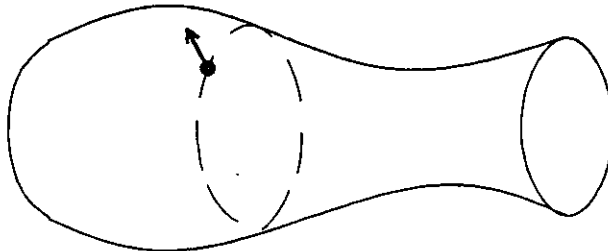
Figure 46: Cross-Section of a Right Circular SHGC Through a Point

As shown in figure 46, the cross-section of the shape through this point, an arc of constant s on the surface, is a circle whose projection in the image is an ellipse. We can determine its equation using x and y. First, we determine:

$$sin\ 2\pi t = \frac{y\ sin\ \sigma}{r(s)} \quad and \quad cos\ 2\pi t = \frac{x - s}{r(s)\ cot\ \sigma}$$

So

$$1 = (\frac{(x - s)\ sin\ \sigma}{r(s)\ cos\ \sigma})^2 + (\frac{y\ sin\ \sigma}{r(s)})^2$$

which is the equation of an ellipse with center at $(s,0)$, vertical semimajor axis of $r(s)\ /\ sin\ \sigma$, and horizontal semiminor axis of $r(s)\ cos\ \sigma\ /\ sin\ \sigma$.

We cannot yet determine the specific paramaters of the ellipse yet, since we do not know s, $r(s)$, or σ. However, we do have a surface normal given by $N = (p, q, 1)$ with p and q defined by equations (4-7) and (4-8) above. Using x, y, p, and q, we can solve for s, t, $r(s)$, and dr/ds all as functions of the unknown viewing angle, σ, for a partially aligned image of an RCSHGC:

$$k = (p\ cos\ \sigma - sin\ \sigma)^2 + q^2 \quad .$$

$$s = \frac{xq - y\ cos\ \sigma\ (p\ cos\ \sigma - sin\ \sigma)}{q}$$

$$t = \frac{1}{2\pi}\ sin^{-1}\ \frac{q}{\sqrt{k}}$$

$$r(s) = \frac{y\ sin\ \sigma\ \sqrt{k}}{q} \quad .$$

$$\frac{dr}{ds} = \frac{-1 - sin\ \sigma\ (p\ cos\ \sigma - sin\ \sigma)}{cos\ \sigma\ k^{1/2}}$$

Thus, given a single surface normal in a partially aligned image, the image of the corresponding cross-section is an ellipse; this ellipse is determined as a function of the viewing angle, σ.

4.7.4 Shadow Geometry for RCSHGCs

In figure 47, we have a line drawing of a Right Circular SHGC, whose shadow is visible and is cast upon a flat surface. If the direction of illumination is known, we can determine the surface normals along the shadow line [17]. This information can be combined with the occluding contour of the RCSHGC, to determine the viewing angle.

We begin by partially aligning the image. Now, select a single point $I = (x,y)_{xpyp}$ along the shadow line. At this point, the surface gradient (p,q) can be obtained.
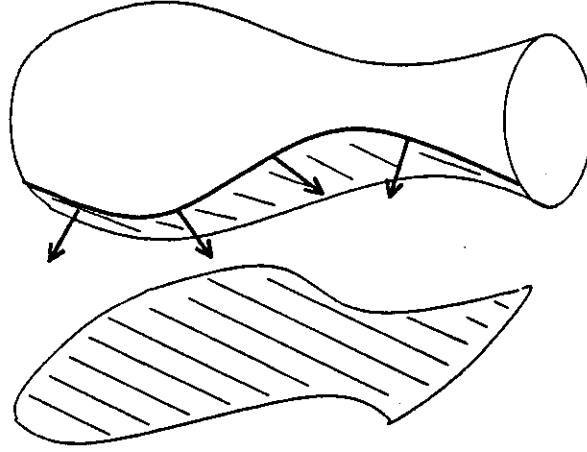
Figure 47: Shadow Geometry Provides Surface Normals Along Shadow Line

For each value of the viewing angle σ, we can compute the implied values of s, t, $r(s)$, and dr/ds at I. Now we can easily derive the following formulas for I_{CGxpyp}, the image of the contour generator in a partially aligned image, from the previously seen equations for I_{CG}, the image of the contour generator in an aligned image:

$$I_{CGxpyp} = (x_{CG}, y_{CG})_{xpyp}$$

$$x_{CG} = -r(s)\cos^2\sigma \frac{dr}{ds} + s$$

$$y_{CG} = \frac{r(s)}{\sin\sigma} \sqrt{1 - \cot^2\sigma \, (dr/ds)^2}$$

$$\frac{dy_{CG}}{dx_{CG}} = \left(1 / \sqrt{\sin^2\sigma - \cos^2\sigma \, (dr/ds)^2}\right) \frac{dr}{ds}$$

Now, if $|\tan\sigma| \geq |dr/ds|$, there must be some point on the contour generator corresponding to the value of s at the given point I (figure 48). At this point, the values of x_{CG}, y_{CG}, and dy_{CG}/dx_{CG} can be determined by substituting for s, $r(s)$, and dr/ds in the above equations, to yield:

$$x_{CG} = x + \frac{y\cos\sigma \, (\sin\sigma + \cos^2\sigma \, [\sin\sigma - p\cos\sigma])}{q}$$

$$y_{CG} = \frac{y \, ([q^2 + 2]\sin^2\sigma - 2p\sin\sigma\cos\sigma - 1)^{1/2}}{q\sin\sigma}$$
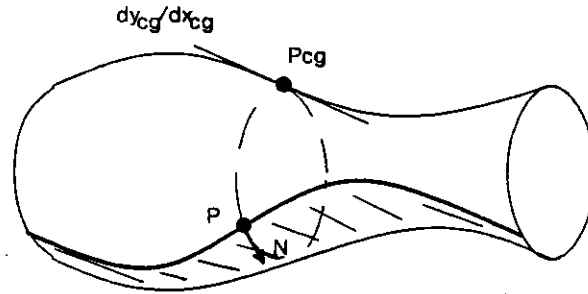
Figure 48: Corresponding Point on Tangency Contour Generator

$$\frac{dy_{CG}}{dx_{CG}} = \frac{-p \sin \sigma - \cos \sigma}{([q^2 + 2] \sin^2 \sigma - 2p \sin \sigma \cos \sigma - 1)^{1/2}}$$

with *k* defined as above.
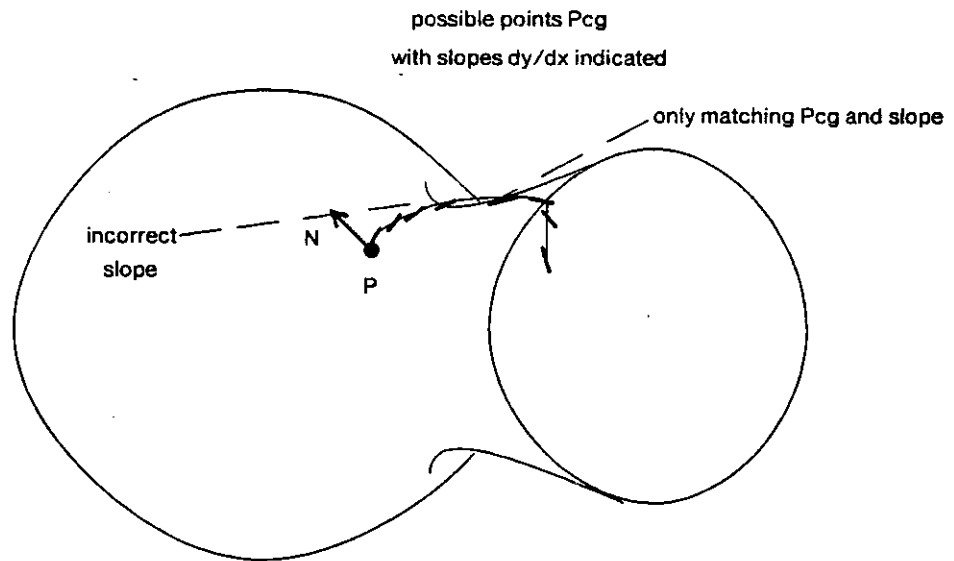
Figure 49: At Most One Corresponding Point Exists

In an image of a Right Circular SHGC, it is guaranteed that at most one point on the occluding contour (and, of course, its reflection about the *x*-axis) will correspond to the same value of *s* as the given point *l*. Thus, it is possible to search along the points (x_{CG}, y_{CG}) for all values of σ, as shown in figure 49, looking for a point which lies on the outline of the shape in the image. There may be more

than one such point on the outline; however, at most one such point will have the correct contour slope dy_{CG}/dx_{CG} in the image. When this point is found, the value of σ which determined it is the viewing angle for image. Full alignment can now be completed, and recovery of $r(s)$ can proceed.

A summary of the process is this: An image of an RCSHGC is partially aligned. Now, given a surface normal at a specific point, the corresponding point (and slope) of the occluding contour for the same value of s can be determined as a function of the viewing angle σ. By searching the image for these points for all values of σ, looking for a crossing of the occluding contour exhibiting the predicted slope, the viewing angle σ can be determined. The image can then be completely aligned for more detailed analysis of the shape.

4.7.5 Range Data Analysis for RCSHGCs
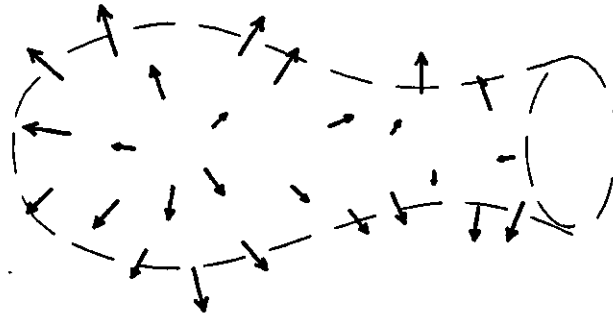
Figure 50: Range Data Yields an Image of Surface Normals

When a range finder is used to produce an image, the result is a set of distances to points in the field of view. By fitting local tangent planes, surface orientations (e.g. gradients) can be determined at many points in the image -- almost at every pixel (but with some gaps, if a common triangulation-based range finder is used) (figure 50). The redundancy provided by such a large number of surface gradients can be used to estimate the viewing angle in a partially aligned image. Here, as above, the discussion will be limited to Right Circular SHGCs for simplicity.

4.7.5.1 Method of Minimizing Derivatives

Suppose we have used a range finder to determine the surface gradient at many points in a partially aligned image of an RCSHGC. For each value of the viewing angle σ, we can compute the corresponding values of s, t, $r(s)$, and dr/ds at each surface normal, using the above formulae.

image x,y,p,q   description r(s)
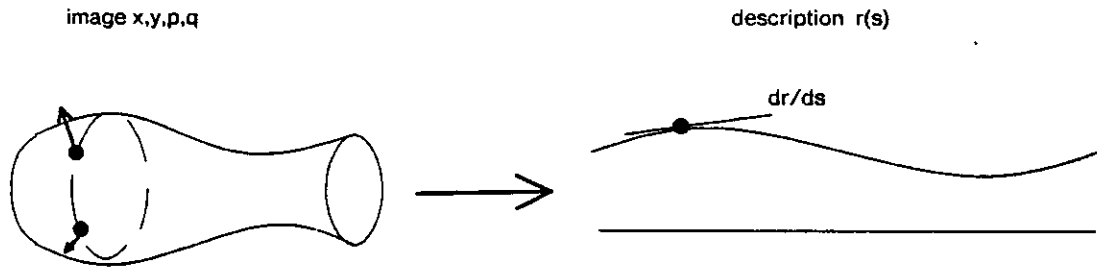
Figure 51: Two Surface Normals on the Same Cross-Section

If we had any two surface normals corresponding to exactly the same value of s, as in figure 51, we could determine the viewing angle as that value of σ for which the two normals produced identical values of s, $r(s)$, and dr/ds. (The authors speculate that this value will be unique.) In general, however, we cannot assume that such a pair of surface normals will be present in the range data. Instead, we can use each pair of surface normals to indicate the value of σ which produces the best consistency between the corresponding estimates of s, $r(s)$, and dr/ds. Then, using some voting scheme, the most preferred value of σ can be selected for performing complete alignment of the image and further analysis of the shape.

image x,y,p,q   description r(s)
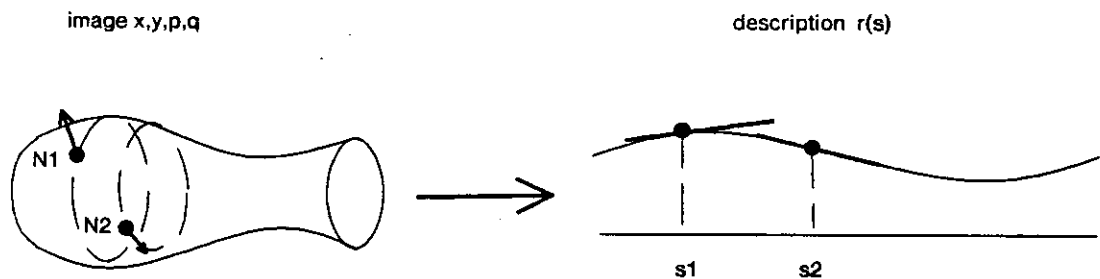
Figure 52: Two Surface Normals on Different Cross-Sections

Consider a pair of points l_1 and l_2 at which the surface gradients (i.e. normals) (p_1, q_1) and (p_2, q_2) are known, as shown in figure 52. For any value of the viewing angle σ, we can compute s_1, $r(s_1)$, $dr/ds\big|_{s1}$, s_2, $r(s_2)$, and $dr/ds\big|_{s2}$. We would like to define a "complexity" measurement for $r(s)$; then, we can determine the value of σ which minimizes this complexity, and say that this value of σ is the value indicated by our pair of surface normals.

Now, for any value of σ, there exist an infinite number of functions $r(s)$ which correspond to the

constraints at s_1 and s_2. A useful kind of complexity might be the highest-order non-zero derivative of $r(s)$: the function $r(s)$ with the fewest non-zero derivatives might be called the "simplest".

With four constaints on $r(s)$ ($r(s)$ at two points, and dr/ds at two points), the function with the fewest non-zero derivatives will be a cubic polynomial, with three non-zero derivatives, of the form:

$$r(s) = as^3 + bs^2 + cs + d$$

with the coeffecients a, b, c, and d determined as in section 4.4.2. Thus, for each value of σ, the coefficients a, b, c, and d can be determined for the cubic polynomial function $r(s)$ relating two surface normals.

We wish to select the value of σ minimizing complexity, i.e. minimizing the number of non-zero derivatives. Thus, we can choose among those cubic functions some "least complex" function, and let the corresponding value of σ be the value indicated by our pair of surface normals. One measure of complexity for these cubics might be $|a|$; since the third derivative $d^3r/ds^3 = 6a$, minimizing $|a|$ is equivalent to minimizing the magnitude of the third derivative of $r(s)$. Ideally, we would hope to find a value of σ for which $|a| = 0$, i.e. a quadratic function $r(s)$ sufficient to account for our pair of surface normals.

Unfortunately, the expression for a is a complicated function:

$$a = \frac{(s_2 - s_1)\,(dr/ds|_{s1} + dr/ds|_{s2}) + 2\,(r(s_1) - r(s_2))}{(s_2 - s_1)^3}$$

Substituting for s, $r(s)$, and dr/ds in terms of σ does not yield any simplification of the above result. Because it seems difficult to find a useful analytic formula for σ, some numeric technique to minimize $|a|$ may be necessary.

On the other hand, not every pair of surface normals need be analyzed. Only those surface normals at points with similar values of s need be considered to provide meaningful constraint; this is equivalent to saying that the assumption that $r(s)$ is quadratic should only be applied locally, over small intervals of s. As an approximation to this criterion, only surface normals at points with similar values of x need be compared (figure 53).

The proposed method for the analysis of range finder images of Right Circular SHGCs is thus: First, fit local surfaces to the range data, to yield an image of surface orientations. Partially align this image. Now examine each pair of surface normals at points within vertical bands of some size (i.e. with similar x-coordinates). For each such pair, determine the value of σ which minimizes $|a|$ (i.e. the
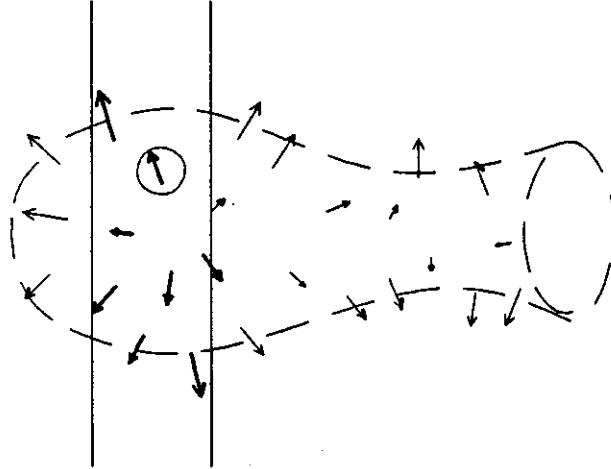
Figure 53: Only Compare Surface Normals with Similar Values of x

magnitude of the third derivative of the cubic approximation to $r(s)$); that pair of surface normals will "vote" for this value of σ, possibly weighted by some confidence measure such as the computed value of $|s_1 - s_2|$. Find the value of σ with the strongest support; assume this is the true viewing angle. Now, the image can be completely aligned for more detailed reconstruction of the RCSHGC description.

While this method involves considerable assumptions about the true nature of the object being observed, it is still significant that the analysis is attempting to minimize a viewpoint-independent measure of the complexity of the object.

4.7.5.2 Method of Interpolating Normals

There is an alternative approach to analyzng range data, which avoids the approximation to $r(s)$ in the previous method, relying instead on a smoothing assumption. In this tecnhique, processing relies on a surface normal interpolation function, capable of determining the (approximate) gradient of the surface normal anywhere in the object's image, by interpolating between known values of the gradient.

With such a function available, whole ellipses can be fit to the data. Consider a surface normal whose gradient (p,q) at a point (x,y) in a partially aligned image is known. Now, for each value of the (unknown) viewing angle σ, not only is the elliptic image of the cross-section through (x,y) determined, but also the gradient at each point on this ellipse is determined (figure 54). For, at any value of t, the corresponding image point (x_t, y_t) and gradient (p_t, q_t) are given by:
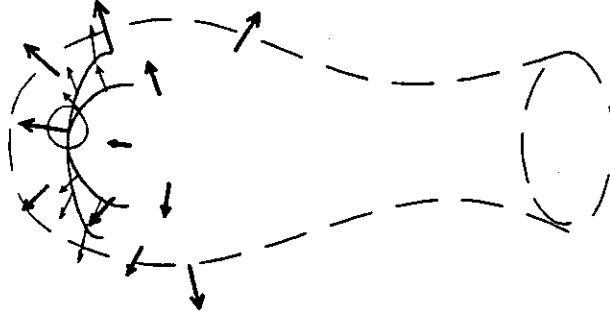
Figure 54: Fitting Ellipses to Interpolated Surface Normals

$$x_t = x + \frac{y \cos \sigma \, (k^{1/2} \cos 2\pi t + \sin \sigma - p \cos \sigma)}{q}$$

$$y_t = \frac{y \, k^{1/2} \sin 2\pi t}{q}$$

$$p_t = -\tan \sigma - \frac{\cos 2\sigma}{\cos \sigma \, (1 + \sin \sigma \, [p \cos \sigma - \sin \sigma + k^{1/2} \cos 2\pi t])}$$

$$q_t = \frac{-k^{1/2} \sin 2\pi t}{1 + \sin \sigma \, (p \cos \sigma - \sin \sigma + k^{1/2} \cos 2\pi t)}$$

where $k = (p \cos \sigma - \sin \sigma)^2 + q^2$. (These are obtained from the formulae in section 4.7.3, substituting the equations for s, $r(s)$, and dr/ds into those for x, y, p, and q.)

At any such point (x_t, y_t), the interpolated gradient (p_i, q_i) can be determined from the interpolation function, using the image data in that neighborhood. An error measure can then be derived to indicate how far the (interpolated) data is from the data predicted from the given point and the assumed viewing angle σ. One such error measure might be the angle between the predicted normal $N_t = (p_t, q_t, 1)$ and the interpolated normal $N_i = (p_i, q_i, 1)$, given by:

$$E(\sigma, t) = \cos^{-1} \frac{N_t \cdot N_i}{\|N_t\| \, \|N_i\|} = \cos^{-1} \frac{p_t p_i + q_t q_i + 1}{(p_t^2 + q_t^2 + 1)^{1/2} (p_i^2 + q_i^2 + 1)^{1/2}}$$

For a given value of σ, an error measure $E(\sigma)$ might be computed by taking the average of $E(\sigma,t)$ over some range of values of t between approx. 1/4 and 3/4 (i.e. on the near side of the object). Note that, for some values of t, the object's surface might be occluded. The point (x,y) used to determine all the values of $E(\sigma)$ might then "vote" for that value of σ which minimizes $E(\sigma)$.

This method for analyzing range finder images is this: First, fit local surfaces to the range data, to yield a (sparse) image of surface orientations. Partially align this image. Now, for each surface normal in some set of surface normals, determine the value of σ which minimizes $E(\sigma)$, the average angle between the surface normals prediced by the selected normal and the interpolated normals determined from the surrounding data. Each of the selected normals will "vote" for the indicated value of σ. Select the value of σ receiving the strongest support; assume this is the true viewing angle. Now, the image can be completely aligned for more detailed analysis.

This method makes weaker assumptions about $r(s)$ than the previous technique, and probably requires less computation. However, it does depend upon the existence of an interpolation function for surface normals, and might also be more sensitive to noise in the data.

5. Conclusions

In this paper, we have presented several kinds of results. First, there have been specific observations and formulae relating to:

- Parameterization of shapes, in particular Straight Homogeneous Generalized Cylinders.
- Theorems about equivalence of descriptions, and behavior of surface normals, for SHGCs.
- Formulae for several attributes of SHGCs, such as coordinates of points, surface normals, and images of these.
- Observations about contour generators, such as planarity and points of singularity. These observations were derived for SHGCs, but in general will apply to more complex shapes as well.
- Analysis techniques for tangency contours and surface normals of Right Circular SHGCs and Right Polygonal SHGCs, including line drawings, images with shadows, and range-finder data.

This work has been theoretical, unaccompanied so far by implementation; it might be thought of as preliminary, exploratory work aimed at outlining goals for eventual implementation efforts.

In addition to these specific observations, a methodology has been produced and demonstrated for analyzing the imaging properties of shapes described parametrically:

1. Parameterize the shape using some set of functions.
2. Parameterize the surface of the shape by s and t.
3. Assign a local (surface-based) coordinate system and find points $P(s,t)$ and surface normals $N(s,t)$.
4. Assign a global (object-centered) coordinate system and convert P and N to global coordinates.
5. Invoke a tangency argument with viewing direction F (in global coordinates) to determine the condition on contour generators.
6. Imbed the object in the world coordinate system $(x\text{-}y\text{-}z)$ with $F = Z$.
7. Determine equations for the images of points $I(s,t)$, note the specialization to tangency contours, and solve for shape parameters in terms of image contours.
8. For surface normal analysis, convert N to world coordinates, solve for gradient (or other representation), solve for shape parameters at arbitrary point in terms of I and image of N.

This methodology is being applied to shapes other than SGCs, in work in progress by the authors.

Finally, it has been discovered that there are several problems whose solutions are very difficult to grasp intuitively; analysis has revealed some important facts not suspected by the authors based on their own intuition. These problems include:

- The conditions for uniqueness or equivalence of shape descriptions.

- The planarity (or lack thereof) for contour generators.
- The conditions under which contour generators exhibit singularities.
- The characterization of the image contours in pictures of even relatively simple shapes.

5.1 Future Work

Although intended applications must guide the direction of future development of such theoretical work as this, there are several open areas already revealed by this research. The analysis of contours has been carried out in some detail for Right Circular SHGCs; it would be useful to extend these results to other types of Generalized Cylinders as well. In addition, no specific algorithms have been suggested for analyzing arbitrary image contours, even if the object being viewed is of a known type. The results will all be more useful when extended to images under perspective projection. The analysis of contour generators from two viewpoints should be able to provide at least some cues as to the solid shape. All of these suggestions pertain to generalizing the results in this paper; in situations where the authors have been daunted by mathematical tractability, the use of some symbol-manipulation system such as MACSYMA might allow for further achievement.

Of equal interest, some considerable space has been devoted in this paper to the description of images and image analysis for Right Circular SHGCs (i.e. solids of revolution), yet several problems are still unsolved. These problems include characterizing and analyzing shading and highlights, analyzing the position of the shadow line in detail, and finding the images of the axis endpoints in an image. This kind of very detailed analysis of simple shapes may yield quite interesting insights for image understanding in general.

Finally, implementation is important as an embodiment of these theoretical results, and for providing feedback for directing further analysis. An important problem to deal with will be that of deciding whether an object is in fact a member of a specific shape class, a problem which is not addressed in this paper.

5.2 Acknowledgements

John Kender at Columbia University provided several useful ideas and helped make the basic definitions more rigorous. Chris Brown at Rochester suggested the torus problem, which led to the formalization of the methodology outlined in the Conclusions.

6. Bibliography

[1]   Ballard, D. H. and Brown, C. M.
        Computer Vision.
        Prentice-Hall, Englewood Cliffs, NJ, 1982.

[2]   Binford, T. O.
        Visual perception by computer.
        In *Proc. IEEE Conf. on Systems and Control.* Miami, December, 1971.

[3]   Brooks, R. A.
        Symbolic reasoning among 3-D models and 2-D images.
        Artificial Intelligence 17:285-348, 1981.
        Special volume on computer vision.

[4]   Davis, H. F. and Snider, A. D.
        Introduction to Vector Analysis, 3rd ed.
        Allyn and Bacon, Boston, 1975.

[5]   Hilbert, D. and Cohn-Vossen, S.
        Geometry and the Imagination.
        Chelsea Publishing Co., New York, 1952.

[6]   Hollerbach, J. M.
        Hierarchical Shape Description of Objects by Selection and Modification of Prototypes.
        AI-TR 346, MIT, November, 1975.

[7]   Horn, B. K. P.
        Understanding Image Intensities.
        Artificial Intelligence 8:201-231, 1977.

[8]   Kanade, T. and Kender, J.
        Mapping Image Properties into Shape Constraints: Skewed Symmetry, Affine-Transformable
            Patterns, and the Shape-from-Texture Paradigm.
        In *IEEE Workshop on Picture Data Description and Management*, pages 130-135. Asilomar,
            CA, August, 1980.

[9]   Kender, J.
        Shape From Texture: A Computational Paradigm.
        In Baumann, L. S. (editor), *Proc. ARPA IUS Workshop*, pages 134-138. April, 1979.

[10]   Kuhl, F. P. and Giardina, C. R.
       Elliptic Fourier features of a closed contour.
       Computer Graphics and Image Processing 18:236-258, 1982.

[11]   Marr, D.
       Analysis of occluding contour.
       Proc. Royal Society of London B-197:441-475, 1977.

[12]   Marr, D. and Nishihara, H. K.
       Representation and recognition of the spatial organization of three-dimensional shapes.
       Proc. Royal Society of London B-200:269-294, 1978.

[13]   Nevatia, R.
       Machine Perception.
       Prentice-Hall, Englewood Cliffs, NJ, 1982.

[14]   Rubinstein, Z.
       A Course in Ordinary and Partial Differential Equations.
       Academic Press, New York, 1969.

[15]   Shafer, S. A., Kanade, T., and Kender, J. R.
       Gradient Space Under Orthography and Perspective.
       In *IEEE Workshop on Computer Vision: Representation and Control*, pages 26-33. August,
           1982.

[16]   Shafer, S. A.
       A Taxonomy of Generalized Cylinders.
       IEEE Transactions on Pattern Analysis and Machine Intelligence , 1983.
       Submitted for Correspondences.

[17]   Shafer, S. A. and Kanade, T.
       Using Shadows in Finding Surface Orientations.
       Computer Graphics and Image Processing , 1983.
       To appear. Also available as technical report from Carnegie-Mellon University Computer
           Science Department.

[18]   Soroka, B. I.
       Generalized cones from serial sections.
       Computer Graphics and Image Processing 15(2):154-166, February, 1981.

I. Symbols

Constants and coordinates are shown in italics (s, W), functions are in boldface italics (r, N). Scalar values are in lower-case (t, u_c), vector or n-tuple values in upper case (G, P), angles in Greek letters (α, σ).

Generalized Cylinders

G	Generalized Cylinder

Classes of Shapes

GC	Generalized Cylinders	LSHGC	Linear SHGCs
SGC	Straight Generalized Cylinders	RSHGC	Right SHGCs
SHGC	Straight Homogeneous GCs	CSHGC	Circular SHGCs
		PSHGC	Polygonal SHGCs

Components of a Generalized Cylinder

$A(s)$	axis function	$E(s,t)$	envelope function
$r(s)$	radius function	$C(t)$	contour function
α	angle of inclination	u_c, v_c	components of contour

Coordinates of a Generalized Cylinder

s	distance along axis	S	axis vector
t	distance along contour	U	horizontal on cross-section
u,v	cross-section coordinates	V	vertical on cross-section
w	normalized u	W	normalized horizontal

Measures of a Generalized Cylinder

$P(s,t)$	point on surface	$N(s,t)$	surface normal
p_w, p_v, p_s	coordinates of point	n_x, n_y, n_z	components of normal
m	slope of $r(s)$ for LSHGC	$h(t)$	contour Wronskian

Projections of Generalized Cylinders

F	viewing direction	X	horizontal in image
f_w, f_v, f_s	viewing direction coordinates	Y	vertical in image
σ	viewing angle (F to S)	Z	direction of eye
L	illumination direction	x,y,z	world and image coordinates
l_w, l_v, l_s	illum. direction coordinates	$I(s,t)$	image of point on SHGC

λ	illumination angle	$x(s,t), y(s,t)$	image coordinates of SHGC point
β	dihedral illumination angle	$\mathbf{G} = (p,q)$	surface gradient

II. Properties of SHGCs

II.1 Straight Homogeneous GC: SHGC

Definition

$G = (A, C, r, \alpha)$

axis $A(s)$ linear

contour $C(t) = (u_C, v_C)(t)$ continuous

radius $r(s)$ differentiable

inclination α constant

Description

GC with straight axis, all cross-section planes parallel, all cross-sections of same shape but varying size.

Point on the Surface

$$P(s,t) = (u_C(t)\, r(s)\, \sin\alpha, \; v_C(t)\, r(s), \; s + u_C(t)\, r(s)\, \cos\alpha)$$

Contour Wronskian

$$h(t) = u_C(t)\frac{dv_C}{dt} - v_C(t)\frac{du_C}{dt}$$

$h(t) = 0$ iff the SHGC can be imbedded in a plane.

Surface Normal

$$N(s,t) = \left(h(t)\cos\alpha\frac{dr}{ds} + \frac{dv_C}{dt}, \; -\sin\alpha\frac{du_C}{dt}, \; -h(t)\sin\alpha\frac{dr}{ds} \right)$$

II.2 Right SHGC: RSHGC

Definition

$$G = (A, C, r, \pi/2)$$

A, C, r as for SHGC.

Description

SHGC with cross-section planes perpendicular to axis.

Special Properties

There is no preferred direction for u and v axes on cross-section planes, so imaging geometry can be simplified. Also, $U = W$.

Point on the Surface

$$P(s,t) = (u_C(t)\, r(s),\ v_C(t)\, r(s),\ s)$$

Contour Wronskian

Same as SHGC -- no simplification.

Surface Normal

$$N(s,t) = \left(\frac{dv_C}{dt},\ -\frac{du_C}{dt},\ -h(t)\frac{dr}{ds} \right)$$

Image of a Point

$$I(s,t) = (x,y)\,(s,t)_{xy} = (u_C(t)\, r(s)\cos\sigma + s\sin\sigma,\ v_C(t)\, r(s))_{xy}$$

World Coordinates

$$P = (w, v, s)_{wvs} = (w\cos\sigma + s\sin\sigma,\ v,\ -w\sin\sigma + s\cos\sigma)_{xyz}$$

Oblique View Contour Generator Condition

$$0 = \sin\sigma\frac{dv_C}{dt} + h(t)\cos\sigma\frac{dr}{ds}$$

Oblique View Contour Generator Domain

Intractable.

Oblique View Contour Generator Point

Intractable.

Oblique View Contour Generator Planarity

Intractable.

II.3 Linear SHGC: LSHGC

Definition

$$G = (A, C, r, \alpha, 0)$$
$$r(s) = m (s - s_0)$$
A, C, α as for SHGC.

Description

SHGC with linear radius function. Apex is at $s = s_0$.

Special Properties:

- *Slant Theorem:* Can describe an LSHGC with cross-section planes at any orientation (as long as they cut completely through shape).

- *Pivot Theorem:* Can describe an LSHGC with any axis passing through apex (excluding projection of shape through apex).

- *Corresponding Normal Theorem:* $\partial N/\partial s = (0,0,0)$

Point on the Surface

$$P(s,t) = (m (s - s_0) u_C(t) \sin \alpha, \; m (s - s_0) v_C(t), \; s + m (s - s_0) u_C(t) \cos \alpha)$$

Contour Wronskian

Same as SHGC -- no simplification.

Surface Normal

$$N(s,t) = \left(m h(t) \cos \alpha + \frac{dv_C}{dt}, \; -\sin \alpha \frac{du_C}{dt}, \; -m h(t) \sin \alpha \right)$$

Right LSHGC:

Image of a Point

$$I(s,t) = (x,y) (s,t)_{xy} = (m (s - s_0) u_C(t) \cos \sigma + s \sin \sigma, \; m (s - s_0) v_C(t))_{xy}$$

Oblique View Contour Generator Condition

$$0 = \sin \sigma \frac{dv_C}{dt} + m h(t) \cos \sigma$$

Oblique View Contour Generator Domain
t_0 satisfying above condition.

Oblique View Contour Generator Point
Intractable.

Oblique View Contour Generator Planarity
Always.

II.4 Circular SHGC: CSHGC

Definition

$G = (A, C, r, \alpha)$

$C(t) = (u_C, v_C)(t) = (\cos 2\pi t, \sin 2\pi t)$

A, r, α as for SHGC.

Description

SHGC with circular cross-section.

Point on the Surface

$P(s,t) = (r(s) \sin \alpha \cos 2\pi t, \ r(s) \sin 2\pi t, \ s + r(s) \cos \alpha \cos 2\pi t)$

Contour Wronskian

$h(t) = 2\pi$

Surface Normal

$$N(s,t) = \left(2\pi \left(\cos 2\pi t + \cos \alpha \frac{dr}{ds} \right), \ 2\pi \sin \alpha \sin 2\pi t, \ -2\pi \sin \alpha \frac{dr}{ds} \right)$$

Right CHGC:

Image of a Point

$$I(s,t) = (x,y)(s,t)_{xy} = (r(s) \cos \sigma \cos 2\pi t + s \sin \sigma, \ r(s) \sin 2\pi t)_{xy}$$

Oblique View Contour Generator Condition

$$t = \frac{1}{2\pi} \cos^{-1} \left(-\cot \sigma \frac{dr}{ds} \right)$$

Oblique View Contour Generator Domain

$$\left| \frac{dr}{ds} \right| \leq | \tan \sigma |$$

Oblique View Contour Generator Point

$$P(s,t) = P_{CG}(s) = \left(\cot \sigma \, r(s) \frac{dr}{ds}, \ r(s) \sqrt{1 - \cot^2 \sigma \, (dr/ds)^2}, \ s \right)$$

Oblique View Contour Generator Planarity

Difficult to evaluate.

Oblique View Contour

$$I_{CG}(s) = (x_{CG}, y_{CG}) (s)_{xy}$$

$$= \left(-r(s) \frac{\cos^2 \sigma}{\sin \sigma} \frac{dr}{ds} + s \sin \sigma, \; r(s) \sqrt{1 - \cot^2 \sigma \, (dr/ds)^2} \right)_{xy}$$

$$\frac{dy_{CG}}{dx_{CG}} = \left(1 / \sqrt{\sin^2 \sigma - \cos^2 \sigma \, (dr/ds)^2} \right) \frac{dr}{ds}$$

Oblique View Contour Analysis

$$s = \frac{x_{CG}(s) - y_{CG}(s) \cos^2 \sigma \, (dy_{CG}/dx_{CG})}{\sin \sigma}$$

$$r(s) = y_{CG}(s) \sqrt{1 + \cos^2 \sigma \, (dy_{CG}/dx_{CG})^2}$$

$$\frac{dr}{ds} = \left(\sin \sigma / \sqrt{1 + \cos^2 \sigma \, (dy_{CG}/dx_{CG})^2} \right) \frac{dy_{CG}}{dx_{CG}}$$

Image of a Surface Normal

$$N(s,t) = \left(\cos \sigma \cos 2\pi t - \sin \sigma \frac{dr}{ds}, \; \sin 2\pi t, \; -\sin \sigma \cos 2\pi t - \cos \sigma \frac{dr}{ds} \right)_{xyz}$$

Surface Gradient

$$G(s,t) = (p,q) (s,t)$$

$$p(s,t) = \frac{\sin \sigma \, (dr/ds) - \cos \sigma \cos 2\pi t}{\sin \sigma \cos 2\pi t + \cos \sigma \, (dr/ds)}$$

$$q(s,t) = \frac{-\sin 2\pi t}{\sin \sigma \cos 2\pi t + \cos \sigma \, (dr/ds)}$$

Surface Normal Analysis

$$k = (p \cos \sigma - \sin \sigma)^2 + q^2$$

$$s = \frac{xq - y \cos \sigma \, (p \cos \sigma - \sin \sigma)}{q \sin \sigma}$$

$$t = \frac{1}{2\pi} \sin^{-1} \frac{q}{\sqrt{k}}$$

$$r(s) = \frac{y \sqrt{k}}{q}$$

$$\frac{dr}{ds} = \frac{-1 - \sin \sigma \, (p \cos \sigma - \sin \sigma)}{\cos \sigma \, k^{1/2}}$$

II.5 Polygonal SHGC: PSHGC

Definition

$$G = (A, C, r, \alpha)$$

$C(t) = (u_C, v_C) (t)$ is piecewise linear

Between vertices, $C(t) = (u_C, v_C) (t) = (m_u t + b_u, m_v t + b_v)$

A, r, α as for SHGC.

Description

SHGC with polygonal cross-section.

Special Properties

Corresponding Normal Theorem: $\partial N/\partial t = (0,0,0)$ on face.

Point on the Surface

$$P(s,t) = ((m_u t + b_u) r(s) \sin \alpha, \ (m_v t + b_v) r(s), \ s + (m_u t + b_u) r(s) \cos \alpha)$$

Contour Wronskian for a Face

$$h(t) = m_v b_u - m_u b_v$$

Surface Normal for a Face

$$N(s,t) = \left(m_v + (m_v b_u - m_u b_v) \cos \alpha \frac{dr}{ds}, \ -m_u \sin \alpha, \ (m_u b_v - m_v b_u) \sin \alpha \frac{dr}{ds} \right)$$

Right PSHGC:

Image of a Point

$$I(s,t) = (x,y) (s,t)_{xy} = ((m_u t + b_u) r(s) \cos \sigma + s \sin \sigma, \ (m_v t + b_v) r(s))_{xy}$$

Oblique View Contour Generator Condition for a Face

$$\frac{dr}{ds} = \frac{m_v \tan \sigma}{m_u b_v - m_v b_u}$$

Oblique View Contour Generator Domain for a Face

s_0 satisfying above condition

Oblique View Contour Generator Point for a Face

Intractable

Oblique View Contour Generator Planarity for a Face

Difficult to determine

Image of a Point on a Crease

$$I(s,t_0) = I_{CG}(s) = (x_{CG}, y_{CG})(s)_{xy} = (u_0\, r(s)\cos\sigma + s\sin\sigma,\ v_0\, r(s))_{xy}$$

Oblique View Contour Analysis for a Crease

$$s = \frac{v_0\, x_{CG}(s) - u_0\, y_{CG}(s)\cos\sigma}{v_0\sin\sigma}$$

$$r(s) = \frac{y_{CG}(s)}{v_0}$$

$$\frac{dr}{ds} = \frac{\sin\sigma\,(dy_{CG}/dx_{CG})}{v_0 - u_0\cos\sigma\,(dy_{CG}/dx_{CG})}$$

A Taxonomy of
Generalized Cylinders

29 November 1982

Steven A. Shafer

Computer Science Department

Carnegie-Mellon University

Abstract

A number of researchers have used generalized cylinders (or generalized cones) for shape representation, but different people have defined these terms in different ways. There has been no standardization of the meaning of these terms, and research results are sometimes limited to subclasses for which there is no terminology.

In this paper, a proposal is made for a definition of Generalized Cylinder, for the definition of a number of interesting subclasses, and for the description of the "ends" of such shapes. A corresponding terminology is presented, including abbreviations for the names of these shape classes. Finally, this terminology is used to compare the shape classes used in past research, and to describe common mathematical shapes such as "solid of revolution".

The views and conclusions contained in this document are those of the authors and should not be interpreted as representing the official policies, either expressed or implied, of the Defense Advanced Research Projects Agency or the US Government.

Table of Contents

ii

List of Figures

1. Introduction

Since the introduction of *generalized cylinders* by Binford in 1971 [3], a number of researchers have used this scheme for representation of solid shapes [1, 6, 7, 8, 9, 11, 12, 13, 14, 15]. However, different people have used the term to refer to somewhat different classes of shapes; indeed, an alternate term, *generalized cone*, has been used by some. There has been no clear-cut definition of these terms which might be universally accepted, nor has there even been a suitable terminology for expressing the different shape classes referred to by different researchers using these terms.

In this paper, a set of terminology is introduced for describing generalized cylinders and several subsets and supersets thereof, along with a notation for naming these shape classes. The presentation takes the form of a taxonomy of shapes.

It is hoped and intended that this set of terms will be sufficiently general to allow the definition and comparison of the various shape classes used in past and present research efforts. To illustrate the sufficiency of this terminology, the shape classes used by several researchers are described using the terms presented herein. Finally, the terms for several common mathematical classes, such as cylinders and solids of revolution, are presented, as defined in this taxonomy.

It is beyond the scope of this work to address such issues as the parameterization of specific shapes, or the existence of multiple descriptions of the same shape. However, this terminology may contribute to the future investigation of these problems by facilitating a precise formulation of the questions involved.

2. The Taxonomy

The taxonomy begins with the definition of Generalized Cylinders. This definition involves four parts: by imposing suitable restrictions on each part, a number of subclasses are defined. By allowing generalizations, supersets are defined.

The terminology uses Generalized Cylinders as a basis; this class of shapes may be abbreviated "GC". Each subclass introduces a new adjective (e.g. "Circular"); the name of that shape class is thus "Circular Generalized Cylinders". Frequently, it will be desirable to cascade such adjectives, as in "Right Circular Generalized Cylinders". Each adjective is normally abbreviated with a single letter; the name of the class may be abbreviated in part or in full, as desired, for example, "RCGC", "Right CGC", "Circular RGC", and "Right Circular Generalized Cylinders" are all terms for the same shape class. (The second and third terms might be useful for emphasizing a particular property of the class in some situations.) The names of shape classes will be capitalized when used to refer to the definitions presented herein.

As noted in the taxonomy, certain restrictions imply others. In such cases, the redundant terms may be omitted. For example, all Circular GCs are also Homogeneous GCs. Thus, "Circular GC" is another name for "Circular Homogeneous GC".

In addition to the basic taxonomy of shapes, definitions are presented for describing the ends of a Generalized Cylinder. These allow a somewhat finer grain of description than the basic terminology.

2.1 Generalized Cylinders

A *Generalized Cylinder (GC)* is defined by four parts:

- There is a space curve, called the *axis* of the shape.

- At each point on the axis, at some fixed angle to the tangent to the axis, there is a *cross-section plane* defined.

- On each such cross-section plane, there a planar curve which constitutes the *cross-section* of the object on that plane.

- There is a *transformation rule* which specifies the transformation of the cross-section as the cross-section plane is swept along the axis. This rule always imposes (at least) the constraint that the cross-section changes smoothly.

The surface of the object is the union of the cross-sections. This is a *generative* definition, rather than a *descriptive* definition, of Generalized Cylinders.

The term *Generalized Cone* may be considered synonymous with Generalized Cylinder, since there has been no clear distinction between the two in the past.

2.2 Subsets of GC

The various subclasses of Generalized Cylinders are formed by imposing restrictions upon the four parts of the definition above.
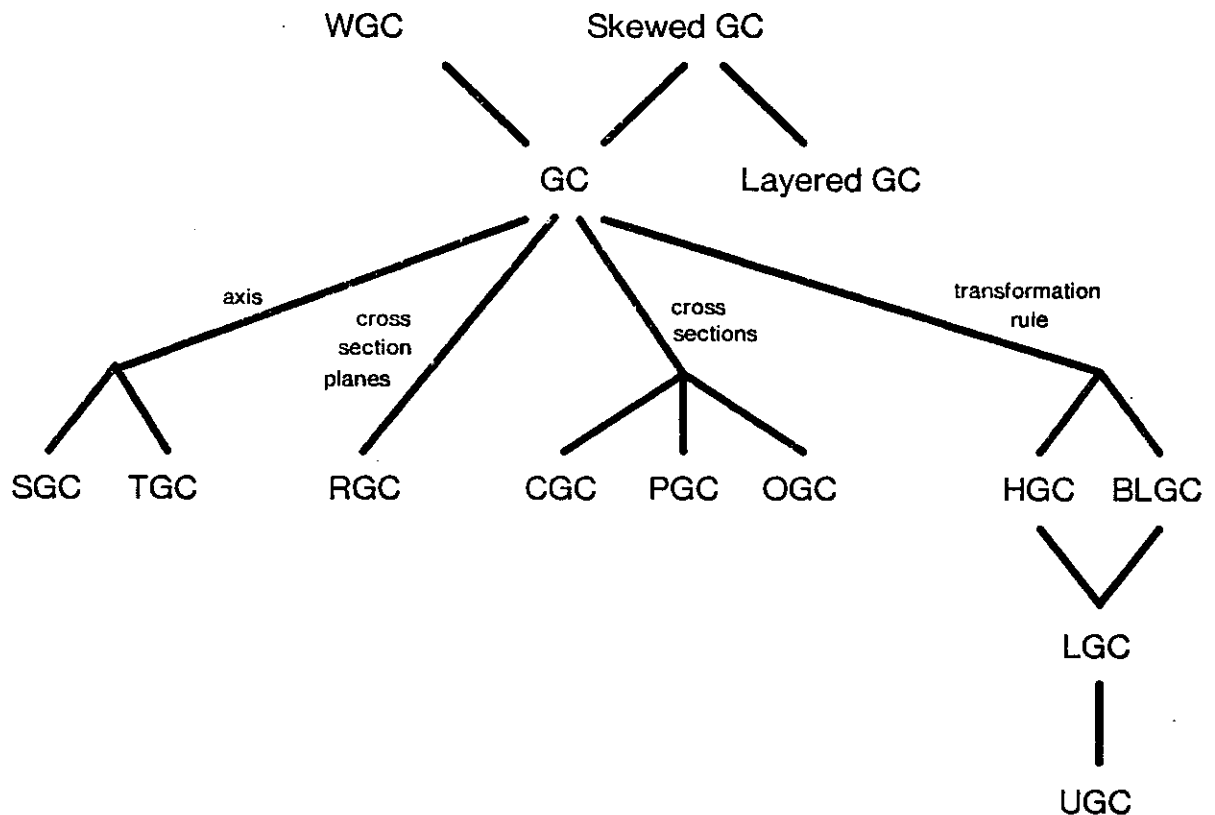

Figure 1: Taxonomy of Generalized Cylinders

The taxonomy is illustrated in Figure 1, in which the nodes are shape classes. The lower classes are subsets of those above them. Adjacent branches are not generally mutually exclusive; thus, the figure is a sort of abbreviated set diagram rather than a strict "tree".

2.2.1 Restricting the Axis

Straight GC (SGC) (opposite: *Curved*)

A Straight Generalized Cylinder has a line segment in space for its axis.

Toroidal GC (TGC) A Toroidal Generalized Cylinder has a closed curve in space as its axis.

2.2.2 Restricting the Cross-Section Planes

Right GC (RGC) (opposite: *Oblique*)

A Right Generalized Cylinder has cross-section planes perpendicular to the tangent to the axis. (In a Straight GC, perpendicular to the axis itself.)

2.2.3 Restricting the Cross-Section

Circular GC (CGC) A Circular Generalized Cylinder has cross-sections which are all circles: Circular GCs are thus also Rounded and Closed (see below). The axis is generally defined to pass through the centers of the circles, in which case the Circular GC is also Homogeneous (see below).

Polygonal GC (PGC) (opposite: *Rounded*)

A Polygonal Generalized Cylinder has cross-sections which are piecewise linear.

Open GC (OGC) (opposite: *Closed*)

An Open Generalized Cylinder has cross-sections which are not Jordan curves, i.e. the cross-section is not a simple closed curve. Usually, an Open GC will have a cross-section which is some arc on the cross-section plane; the shape is thus a piece of a warped sheet in space.

2.2.4 Restricting the Transformation Rule

Homogeneous GC (HGC) (opposite: *Heterogeneous*)

A Homogeneous Generalized Cylinder has a transformation rule which allows only uniform scaling of the cross-section as it is swept along the axis; thus, all cross-sections have the same *shape*, but may vary in *size*.

Linear GC (LGC) A Linear Generalized Cylinder is a Homogeneous Generalized Cylinder in which the size of the cross-section is proportional to distance along the axis, measured from some point called the *apex* of the shape.

Uniform GC (UGC) A Uniform Generalized Cylinder is a Linear Generalized Cylinder in which all cross-sections are identical in size as well as shape.

Bilinear GC (BLGC)

A Bilinear Generalized Cylinder is a Generalized Cylinder in which the cross-section size varies with distance from the apex, but the two orthogonal directions on the cross-section planes have different factors of proportionality, i.e. the cross-section shape is scaled differently in the two directions.

2.3 Supersets of GC

The following are generalizations of Generalized Cylinders:

Warped GC (WGC) A Warped Generalized Cylinder is defined in a similar manner to a Generalized Cylinder, but the cross-sections need not be planar. The cross-sections are thus space curves defined relative to the cross-section planes, but need not be contained within them. This is the class of shapes originally defined as "generalized cylinders" by Binford [3]. It may be interesting to discover whether each shape that is a Warped GC may also be described as a GC (aside from the obvious difference in the planarity of the ends of the shape); if so, WGC = GC. The author conjectures that this is true.

Skewed GC A Skewed Generalized Cylinder is defined similarly to a Generalized Cylinder, but the cross-section planes need not all be at the same angle with respect to the axis. This allows "rotational sweeps" of the cross-section planes, as well as translation of the cross-section planes along the axis.

Layered GC A Layered Generalized Cylinder is a Skewed GC in which the cross-section planes, while not at a fixed angle to the axis, are parallel to each other. This situation arises, for example, when examining serial sections of Curved GCs. Layered GCs do not actually constitute a superset of GCs: a Layered GC with a straight (linear) axis is a Straight GC; whereas a Layered GC with a non-linear axis is a Skewed GC but not a GC.

2.4 Describing the Ends of a Generalized Cylinder

Each end of a Generalized Cylinder may be characterized, independently of the characterization of the shape as a whole.

Blunt An end of a GC is Blunt if the surface normals converge in orientation to be perpendicular to the final cross-section plane at that end (i.e. the surface smoothly approaches the final cross-section).

Flat An end of a GC is Flat if it is not Blunt, and the final cross-section is a closed

curve. The surface normals are discontinuous along the final cross-section, i.e. between the side(s) of the shape and the Flat end.

Chiseled   An end of a GC is Chiseled if it is not Blunt, and the final cross-section is an arc. The surface normals are discontinuous along the final cross-section arc.

Pointed   An end of a GC is Pointed if it is not Blunt and if the final cross-section consists of a single point. The surface normal at this point is undefined.

It is especially interesting to note that a Linear GC always has one end Flat, and the other end may be either Flat or Pointed (but not Blunt or Chiseled). A Uniform GC always has two Flat ends. A Bilinear GC may have one Flat and the other Flat, Chiseled, or Pointed; or it may have both ends Chiseled. The ends of other GCs may be of any type.

3. Application of the Taxonomy

3.1 Common Mathematical Shape Classes

This terminology can be used to define several common mathematical shape classes. In general, the terms used to restrict those mathematical classes are the same terms presented here for restricting the class of Generalized Cylinders (i.e. Right, Circular).

cylinder
A *cylinder* is a Straight Uniform Generalized Cylinder, i.e. SUGC. Subclasses: right, circular.

cone
A *cone* is a Non-Uniform Straight Linear GC (Non-Uniform SLGC), with one end (the apex) Pointed. Subclasses: right, circular.

frustrum
A *frustrum* is a Non-Uniform Straight Linear GC (Non-Uniform SLGC) with both ends Flat.

solid of revolution
A *solid of revolution* is a Straight Right Circular Generalized Cylinder (SRCGC).

parallelopiped
A *parallelopiped* is a Straight Uniform Polygonal Generalized Cylinder (SUPGC). Subclasses: right.

pyramid
A *pyramid* is a Non-Uniform Linear Polygonal Straight Right Generalized Cylinder (Non-Uniform LPSRGC), with one end Pointed.

torus
A *torus* is a Uniform Right Toroidal Generalized Cylinder (URTGC). The shape of the axis and the cross-section must be described separately; in this terminology, a "Circular URTGC" implies that the cross-section is circular, but does not constrain the axis to be a circle.

2-1/2 D shape
The *two-and-a-half-D shape* class used in CAD/CAM is somewhat loosely defined, but usually consists of two polygonal faces linked by quadrilateral or triangular facets [5]. This corresponds to Polygonal Straight GCs with Flat ends, usually Right, but possibly Oblique and with nonparallel ends. Sometimes, shapes with curved axes are also called 2-1/2 D shapes. This type of shape should not be confused with the *2-1/2 D sketch*, a representational scheme used by Marr [9].

3.2 Shape Classes Used in Past Research

The terms *generalized cylinder* and *generalized cone* have been used in past research, to refer to various shape classes. Binford [3] defined "generalized cylinders" to be the class here called Warped GCs. Agin [1] defined the term similarly, but his results were limited to Right Circular Linear GCs, i.e. those with circular cross-section perpendicular to the axis, and linear scaling of the cross-section, but with any space curve as axis. Hollerbach [7] defined "generalized cylinder" as RGC, and limited his attention to HRGCs whose axes were planar (but not necessarily straight). Ballard and Brown [2] defined "generalized cylinder" to be Closed GC, i.e. GCs with cross-sections which are closed arcs; Shani [13] defined "generalized cylinders" as Closed RGCs, i.e. GCs with cross-sections which are closed arcs and lie at right angles with the axis.

Nevatia and Binford [11], and Miyamoto and Binford [10], used the term "generalized cone" to indicate Right GCs, i.e. GCs with cross-sections perpendicular to the axis. Marr and Nishihara [9] used the same term to indicate Homogeneous GCs, those whose cross-sections have constant shape but varying size, but Marr in [8] added the restriction that the axis be straight (i.e. SHGCs). Woodham [15] also referred to SHGCs as "generalized cones".

In describing the ACRONYM program, Brooks [6] uses the term "generalized cone", defined (as here) to be GC. The program's repertoire of shapes, however, is limited to those GCs which are:
1. Either Circular or Polygonal.
2. Bilinear (including Linear and Uniform as special cases).
3. Either Straight; or Right Toroidal with circular axis.

However, Brooks' co-researcher Binford [4] uses the term "generalized cylinder" to refer to ACRONYM's shape descriptions.

Soroka [14] defined "Elliptical Cones" to be SBLGC with elliptical cross-sections; i.e. GCs with straight axes and elliptical cross-sections scaled independently (but linearly) in two orthogonal directions. Soroka allowed both Right and Oblique GCs.

In research related to this paper, Shafer and Kanade [12] use the terminology described herein. Their attention is limited to Straight Homogeneous GCs, for which they present fundamental theorems derived from the definition, and an analysis of image contours and surface normals for SHGCs.

4. Summary

This paper is intended to be a step towards the development of a precise set of terms to be used for describing shape classes. These might be used to compare or describe the classes of shapes dealt with by various researchers; they might even be used to help formulate some of the more difficult problems involved in shape description.

To this end, a taxonomy and terminology have been presented for the shapes known as *generalized cylinders*. The taxonomy begins with the definition of Generalized Cylinders, and includes subsets and supersets of this class of shapes. The terminology introduces terms and abbreviations for each shape class.

Common mathematical shape classes are equivalent to some of these classes, and the shapes dealt with by other researchers can be described in this terminology. Doing so may allow the reader to better understand what assumptions have been made in various research efforts.

4.1 Acknowledgements

5. Bibiography

[1]   Agin, G. J. and Binford, T. O.
        Computer Description of Curved Objects.
        IEEE Trans. on Computers C-25:439-449, April, 1976.

[2]   Ballard, D. H. and Brown, C. M.
        Computer Vision.
        Prentice-Hall, Englewood Cliffs, NJ, 1982.

[3]   Binford, T. O.
        Visual perception by computer.
        In *Proc. IEEE Conf. on Systems and Control.* Miami, December, 1971.

[4]   Binford, T. O.
        Spatial Representation.
        In Baumann, L. S. (editor), *Proc. ARPA IUS Workshop*, pages 140-143. November, 1979.

[5]   Braid, I. C.
        Designing with volumes.
        PhD thesis, Computer Aided Design Group, University of Cambridge Computer Laboratory,
            1973.

[6]   Brooks, R. A.
        Symbolic reasoning among 3-D models and 2-D images.
        Artificial Intelligence 17:285-348, 1981.
        Special volume on computer vision.

[7]   Hollerbach, J. M.
        Hierarchical Shape Description of Objects by Selection and Modification of Prototypes.
        AI-TR 346, MIT, November, 1975.

[8]   Marr, D.
        Analysis of occluding contour.
        Proc. Royal Society of London B-197:441-475, 1977.

[9]   Marr, D. and Nishihara, H. K.
        Representation and recognition of the spatial organization of three-dimensional shapes.
        Proc. Royal Society of London B-200:269-294, 1978.

[10] Miyamoto, E. and Binford, T. O.
      Display Generated by a Generalized Cone Representation.
      In *Conf. on Computer Graphics, Pattern Recognition, and Data Structure*, pages 385-387.
          IEEE Computer Society and ACM SIGGRAPH, May, 1975.

[11] Nevatia, R. and Binford, T. O.
      Description and recognition of curved objects.
      Artificial Intelligence 8:77-98, 1977.

[12] Shafer, S. A. and Kanade, T.
      The Theory of Straight Homogeneous Generalized Cylinders.
      Technical Report, Carnegie-Mellon University, Computer Science Department, 1982.
      In preparation.

[13] Shani, U.
      A 3-D model-driven system for the recognition of abdnominal anatomy from CT scans.
      In *International Joint Conf. on Pattern Recognition*, pages 585-591. Miami Beach, Florida,
          December, 1980.

[14] Soroka, B. I.
      Generalized cones from serial sections.
      Computer Graphics and Image Processing 15(2):154-166, February, 1981.

[15] Woodham, R. J.
      Reflectance Map Techniques for Analyzing Surface Defects in Metal Castings.
      PhD thesis, MIT AI Lab, June, 1978.
      Available as MIT AI-TR-457.